OXFORD UNIVERSITY PRESS | **Journal of Antimicrobial Chemotherapy**

The relative rate of kill of the MMV Malaria Box compounds provide links to the mode of antimalarial action and highlight scaffolds of medicinal chemistry interest

SCHOLARONE™ Manuscripts

1   **The relative rate of kill of the MMV Malaria Box compounds provide**

2   **links to the mode of antimalarial action and highlight scaffolds of medicinal**

3   **chemistry interest**

4

5   **Imran ULLAH^1, Raman SHARMA[2], Antonio METE[3], Giancarlo A. BIAGINI[2], Dawn M.**

6   **WETZEL[4] and Paul D. HORROCKS*[1]**

7   [1]Institute for Science and Technology in Medicine, Keele University, Staffordshire ST5 5BG,

8   United Kingdom; [2]Research Centre for Drugs and Diagnostics, Liverpool School of Tropical Medicine,

9   Pembroke Place, Liverpool L3 5QA, United Kingdom; [3]Medsyndesign Ltd, Advanced Technology

10   Innovation Centre, 5 Oakwood Drive, Loughborough, LE11 3QF, United Kingdom; [4]Department of

11   Pediatrics, University of Texas Southwestern Medical Center, Dallas, 75235 Texas, USA

12

13   *Corresponding author. Institute for Science and Technology in Medicine, Keele University,

14   Staffordshire ST5 5BG, United Kingdom.

15   Tel: +44-(0)-1782-733670

16   E-mail: p.d.horrocks@keele.ac.uk

17   **Running title:** Antimalarial relative rate of kill

18

^ Current address: Department of Pediatrics, University of Texas Southwestern Medical Center, Dallas, 75235 Texas, USA

Abstract

Objectives: Rapid rate-of-kill (RoK) is a key parameter in the target candidate profile 1 (TCP1) for the next-generation antimalarial drugs for uncomplicated malaria, termed Single Encounter Radical Cure and Prophylaxis (SERCaP). TCP1 aims to rapidly eliminate the initial parasite burden, ideally as fast as artesunate, but minimally as fast as chloroquine. Here we explore whether the relative RoK of the Medicine for Malaria Venture (MMV) Malaria Box compounds are linked to their mode of action (MoA) and identify scaffolds of medicinal chemistry interest.

Methods: We used a Bioluminescence Relative RoK (BRRoK) assay over 6 and 48h, with exposure to equipotent-IC_{50} concentrations, to compare the cytocidal effects of Malaria Box compounds to benchmark antimalarials.

Results: BRRoK assay data demonstrate the following relative RoK from fast to slow: inhibitors of *Pf*ATP4 > parasite hemoglobin catabolism > DHFR-TS > DHODH > bc1 complex. Core scaffold clustering analyses reveal intrinsic rapid cytocidal action for diamino-glycerols and 2-(aminomethyl)phenol, but slow action for 2-phenylbenzimidazoles, 8-hydroxyquinolines, and triazolopyrimidines.

Conclusion: This study provides proof of principle that a compound's RoK is related to its MoA, and target's intrinsic RoK is also modified by factors affecting a drug's access to it. Our findings highlight that as we use medicinal chemistry to improve potency, we can also improve the RoK for some scaffolds. Our BRRoK assay provides the necessary throughput for drug discovery and a critical decision-making tool to support development campaigns. Finally, two scaffolds, diamino-glycerols, and 2-phenoxybenzylamine, exhibit fast cytocidal action, inviting medicinal chemistry improvements towards TCP1 candidates.

Introduction

44

45   Resistance by *P. falciparum* to front-line therapeutics necessitates new drugs with novel

46   MoA to circumvent parasite resistance mechanisms.[1,2] This need was initially met by the

47   identification of 20,000 hits with sub-micromolar potency against *P. falciparum* intraerythrocytic

48   stages from an extensive screening campaign of around four million compounds from the libraries of

49   St. Jude Children's Research Hospital, TN, USA, Novartis and GSK. [2–6] Triaging these hits to establish

50   development priorities requires additional pharmacodynamic information, key amongst which is

51   their rate-of-kill (RoK).[7] Rapid RoK is specifically identified by MMV as a key requirement within a

52   future SERCaP to treat malaria.[1,8] The target candidate profile TCP1 requires an immediate effect to

53   rapidly eliminate parasites, minimally as fast as chloroquine and ideally as fast as artesunate. If

54   resistance renders artemisinin ineffective, TCP1 candidates will ideally replace it.[1,8]

55   Antimalarial RoK is currently determined *in vivo* with mouse models or phase IIa clinical

56   trials.[9] It is defined by (i) the parasite reduction ratio (PRR), the fold-reduction from starting

57   parasitaemia after 48 hours (h, one erythrocyte-stage cycle) of treatment and (ii) parasite clearance

58   time (PCT), time until parasites are no longer detectable in peripheral blood films[9]. The only *in vitro*

59   RoK assay that provides the PRR and PCT parameters is the recrudescence assay at GSK Tres

60   Cantos,[10] representing the gold-standard for RoK determination *in vitro*. However, its challenging

61   technical aspects, such as requirements for parasite recrudescence over 21-28-days, limit

62   applicability to small-scale lead validation.[7,11–13] To address this assay bottleneck, we reported a

63   microplate-based BRRoK assay that discriminates between minimum essential and ideal TCP1

64   candidates within 6h (BRRoK[6h]), [10] and published RoK data for 370 open-access Medicine for Malaria

65   Venture's Malaria Box compounds relative to a panel of known antimalarial benchmarks. [2,7] In this

66   study, we extend this study of RoK for the Malaria Box compounds to demonstrate the following

67   proof-of-principles. First, to show that compounds with similar BRRoK have similar MoA, we

68   compared BRRoK[6h] from Malaria Box compounds to their predicted MoA. Five clusters emerged,

69   with each representing distinct relative RoK correlating with different MoA. Second, to demonstrate

70   that Malaria Box compounds with related scaffolds have similar rates of antimalarial killing, BRRoK[6h]

71   were compared based on compounds' core scaffold with five clusters emerging that we then

72   correlated with what we know about potential MoA. Third, we had previously identified 178 Malaria

73   Box compounds that showed little cytocidal activity within 6h.[10] Thus, we extended the assay over

74   48h (BBRoK[48h]) to ensure completion of one intraerythrocytic cycle. Most compounds without

75   activity in the BRRoK[6h] showed activity in the BRRoK[48h], providing links to their MoA. Our data

76   demonstrates that a revised BRRoK assay at two timepoints, 6 and 48h, provides a critical decision-

77   making tool for antimalarial drug discovery and development campaigns.

79 **Methods**

80   The transgenic Dd2 *P. falciparum* clone (Dd2^{luc})[14,15] were cultured as described previously.[7]

81 The antimalarial drugs and the Malaria Box compounds were prepared as shown in Table S1. Malaria

82 Box IC$_{50}$ were measured in Dd2^{luc} and deposited in the ChEMBL − Neglected Tropical Disease Open

83 Access repository (ChEMBL3392923, see Van-Voorhis *et al.,*[16]).

84   The BRRoK^{48h} assay was carried out as described previously[7]. Briefly, compounds were

85 serially diluted (9× IC$_{50}$, 3x IC$_{50}$, 1x IC$_{50}$ and 0.3× IC$_{50}$ concentrations from a determination of IC$_{50}$ at

86 48h) in 96-multiwell plates, trophozoite-stage (20–26 h post-infection) cultures of Dd2^{luc} were added

87 and mixed by pipetting to give a final 200 μL volume in each well with 3-fold IC$_{50}$ dilution series of

88 drugs, 1% parasitaemia and 2% haematocrit. To estimate the BRRoK^{48h}, the plates were incubated

89 continuously in the presence of the compounds for 48h prior to assay at 37°C. As described

90 previously, [7,17] 40 μL of *P. falciparum* culture were transferred to a white 96-multiwell plate (Greiner,

91 UK) and lysed with 10 μL of passive lysis buffer (Promega, UK). An equal volume, 50 μL, of the

92 supplied luminogenic substrate was mixed with the lysed parasites and the bioluminescence was

93 measured for 2 s in a Glomax-Multi Detection System (Promega, UK). Experiments were carried out

94 as technical triplicates on the same plate, with three independent biological repeats of each plate

95 performed. Controls in each biological replicate consisted of trophozoite-stage culture with no drug

96 added (100%) or uninfected erythrocytes (0%). The mean and standard deviation (SD) of

97 bioluminescence data from three independent biological repeats were expressed as a proportion of

98 the untreated control (100%) and calculated as follows: $100 \times [\mu(S) - \mu(-)/\mu(+) - \mu(-)]$, where $\mu(S)$,

99 $\mu(+)$ and $\mu(-)$ represent the means for the sample in question and 100% and 0% controls,

100 respectively. The Z' score of the BRRoK^{48h} assay was calculated as follows: $Z' = 1 -$

101 $[(3\sigma_{(+)} + 3\sigma_{(-)})/\mu_{(+)} - \mu_{(-)}]$, where $\mu_{(+)}$ and $\sigma_{(+)}$ are the mean and SD of the no-drug (untreated) positive

102 control, respectively, and $\mu_{(-)}$ and $\sigma_{(-)}$ are the mean and SD from uninfected erythrocytes (negative

103 control), respectively.[18] The signal/background (S/B) ratio was calculated as follows: $[\mu_{(+)} - \mu_{(-)}]/\sigma_{(-)}$.

104   As previously described,[7] a principle components analysis (PCA) was performed on the BRRoK assay

105   data for the MMV Malaria Box compounds (48h assays using a $9\times IC_{50}$, $3x\ IC_{50}$, $1x\ IC_{50}$ and

106     $0.3\times IC_{50}$ series) using the KNIME analytics platform, to reduce the dimensionality of these data

107   sets[19], allowing the concentration-rate relationship to be captured in one parameter. The first

108   principle component (PC1) accounted for 78% of the total variance of the data (see supplementary

109   materials). A zero-meaned PC1 value is used to provide a description of the RoK relative to known

110   antimalarial benchmark controls (see Table S1).[7]

Results

The BRRoK[6h] for the Malaria Box identifies compound clusters linked by common modes of

antimalarial action

That antiplasmodial *in vitro* RoK correlates with MoA has been established for a small number of antimalarial drugs, predominantly within classes that have been or are currently used.[10] We have previously described a determination of the rates of initial cytocidal kill (over 6h) using the Bioluminescence Relative Rate of Kill (BRRoK) assay for 370 compounds from the Malaria Box open-access drug discovery resource relative to a range of benchmark antimalarials for which both *in vitro* and *in vivo* rates of kill data were available.[7] This determination used *a P. falciparum* strain genetically modified to express a bioluminescent luciferase reporter protein, with cytocidal action determined by loss of bioluminescent signal following exposure to increasing concentrations of test compound. Analysis of the normalised concentration-dependant bioluminescent signals by principle components analysis provides for a rank of initial cytocidal action that enables rate of kill relative to known controls to be described. Termed PC1, for first principle component, these are presented as zero-meaned data where low values such as -97.4 relate to the extremely rapid acting dihydroartemisinin and higher values, such as 55.4, for the slow-acting atovaquone.[7]

With BRRoK[6h] data for 370 Malaria Box compounds, we correlated these with MoA data made available as part of this open source drug discovery project (Figure 1).[20–34] PC1 were plotted against their IC_{50} (ChEMBL3392923, see Van-Voorhis *et al.,*[16]) and mapped against benchmark antimalarials. Compounds with RoK ≥ dihydroartemisinin (DHA, PC1= -97.4) and ≥ chloroquine (CQ, PC1 = -73.7, log PRR= 4.5, 99% PCT= 32h) meet the TCP1 ideal and minimum essential criteria, respectively. Generally, compounds with RoK ≥ CQ are considered fasting acting, those with a RoK ≥ Quinine (QN, PC1 = -52), Mefloquine (MQ, PC1 = −42.4, log PRR = 3.7 and 99.9% PCT = 43 h) or Piperaquine (PQ, PC1 = -37, log PRR = 4.6, 99% PCT = 33h) are considered moderate acting, and those with RoK ≥ Atovaquone (ATQ, PC1 = 55.4, log PRR = 2.9 and 99.9% PCT = 90 h) are slow-acting

137   (Figure 1, S1 Table). Thus, compounds with an initial rapid RoK and nM potency, like artemisinins,

138   occupy the bottom-left quadrant those such as atovaquone, whilst potent, being slow-acting

139   occupies the upper left-hand quadrant (Figure 1).

140   MoA data was sourced from specific activity assays (e.g. *in vitro* enzyme inhibition assays) to

141   comparative metabalomic profiling, and as such the MoA association for the Malaria Box are often

142   tentative. We hypothesized that compounds with a shared MoA would exhibit similar BRRoK^{6h} data.

143   Five MoA including compounds targeting (i) *Pf*ATP4, a Na$^+$-ATPase in the parasite's plasma

144   membrane, ii) bifunctional *Plasmodium* enzyme dihydrofolate reductase-thymidylate synthase

145   (DHFR-TS), (iii) dihydroorotate dehydrogenase (DHODH), (iv) the bc$_1$ complex of the mitochondrial

146   electron transport chain and (v) parasite hemoglobin catabolism (Figure 1A-E) were clustered. These

147   MoA were selected because *in vitro* PRR data are available for $\geq$ 10 compounds (Table S2) in each

148   class.[16,20,21,27,28,35] RoK were identified from fast to slow: *Pf*ATP4 > parasite hemoglobin catabolism >

149   DHFR-TS > DHODH > bc1 complex. Using one-way ANOVA with a post-hoc Tukey test [7,16,20,29,30], we

150   found that compounds targeting *Pf*ATP4 exhibit the fastest RoK and are significantly faster than

151   other clusters (Figure 1F). Compounds targeting parasite hemoglobin catabolism are significantly

152   faster than those targeting DHFR-TS, DHODH and bc$_1$ complex, and compounds targeting DHFR-TS

153   are faster than DHODH and bc1 complex inhibitors (all *p* < 0.01), while other pairwise comparisons

154   are not significant.

155   **BRRoK^{6h} highlights rapid cytocidal activity for diamino-glycerols and 2-(aminomethyl)phenol**

156   **scaffolds in the Malaria Box**

157   The Malaria Box compounds were selected to be structurally diverse.[2] We wished to

158   determine whether substructure analysis of these novel Malaria Box compounds reveals novel core

159   scaffolds with shared RoK activity, and thus potentially with new MoA. BRRoK^{6h} data was overlaid

160   with five distinct scaffolds; diamino-glycerols, 2-(aminomethyl)phenol, 2-phenylbenzimidazole, 8-

161   hydroxyquinolines, and triazolopyrimidine (Figure 2). Table S3 shows full structures and the core

162   scaffold substructures, with $\geq$ 5 compounds for each scaffold annotated. We found a fast BRRoK for

163   diamino-glycerols and 2-(aminomethyl)phenols, and slow BRRoK for 2-phenylbenzimidazoles, 8-

164   hydroxyquinolines and triazolopyrimidines (Figure 2A-E). The five core scaffolds identified BRRoK

165   ranking from fast to slow: diamino-glycerols > 2-(aminomethyl)phenol > 2-phenylbenzimidazole > 8-

166   hydroxyquinolines > triazolopyrimidine. The diamino-glycerol scaffold exhibited the fastest cytocidal

167   action among the group ($p < 0.01$ for all, except 2-(aminomethyl)phenol where $p > 0.05$ by ANOVA

168   (Figure 2F). Similarly, compounds in the 2-(aminomethyl)phenol scaffold exhibited significantly faster

169   action ($p < 0.01$) than the 2-phenylbenzimidazole, 8-hydroxyquinolines and triazolopyrimidine

170   scaffolds (Figure 2F).

171   **BRRoK[48h] confirms slow cytocidal action for a subset of compounds in the Malaria Box**

172   The BRRoK[6h] assay identified fast-acting Malaria Box compounds as TCP1 candidates,

173   including the fastest-acting *Pf*ATP4 inhibitor spiroindolone MMV396749 (Table S2). However, almost

174   half of the Malaria Box showed little cytocidal activity against intraerythrocytic trophozoites over 6h.

175   We predicted that these compounds might have a lag phase in their cytocidal action, such as shown

176   by the antimalarial atovaquone with a 48h lag in cytocidal action.[10] We therefore employed a revised

177   BRRoK assay over 48h (BRRoK[48h]) to ensure completion of one full intraerythrocytic cycle. For

178   validation, we selected different benchmark antimalarials, which covered multiple MoA.[7] Dd2[luc]

179   parasites were exposed to a 3-fold serial dilution ($9–0.33 \times IC_{50}$) for 48h, the resulting

180   bioluminescence signal normalized to an untreated control, and the normalized bioluminescent

181   signal plotted against drug concentration (Figure S1). We found the identical relative ranking order

182   of   benchmark   antimalarial   drugs   (i.e.   artemisinin > chloroquine > 4-

183   methanolquinolines > atovaquone) to   BRRoK[6h],[7] which is identical to both the *in vivo* and *in*

184   *vitro* RoK.[31–33,35]

185   We had sufficient material available for 178 slow-acting Malaria Box compounds. Along with the

186   benchmark antimalarial drugs ATQ, CQ, DHA, MQ, PPQ, pyronaridine (PYN) and QN, we subjected

187 them to a BRRoK^{48h} assay (Table S4; Figures S2, S3). 95% confidence intervals for the Z' score (0.85-

188 0.95), maximum coefficient of variation (0.9%-2.84%), and signal/background ratio (2580-5001)

189 indicate a robust and sensitive microplate-based assay of the BRRoK^{48h} data. Using mean ± SD for

190 each IC$_{50}$-fold BRRoK^{48h} normalized bioluminescent signal, a PCA was carried out for concentration-

191 dependent effects (Figure S4; Tables S5-S6). PC1 accounts for 78% of the variance at 48h, with most

192 contributions provided by the 3X IC$_{50}$ data.

193   We next plotted BRRoK^{6h} and BRRoK^{48h} PC1 against IC$_{50}$ data (Figure 3, Table S7). Figure 3A

194 highlights these compounds' slow action over 6 h, with compounds clustering adjacent to the slow

195 acting atovaquone. Plotting BRRoK^{48h} data against IC$_{50}$ results in a wide distribution of 48h RoK for

196 these compounds (Figure 3B). Interestingly a number of initially slow acting compounds now show a

197 48h RoK within the TCP1 target range (>chloroquine) and presumably reflect a shorter lag phase in

198 their action, such as the 24hr lag phase reported for pyrimethamine.[10] The majority of compounds,

199 however, still show a BRRoK PC1 more similar to atovaquone, and thus potentially a longer lag

200 phase. To explore this, compounds with two predicted slow-acting MoA[16,20,22–26,29,30,34,36–39] were

201 correlated with BRRoK^{48h}; 38 were DHODH inhibitors (Figure 4A, Table S7) and 18 were bc$_1$ complex

202 inhibitors (Figure 4B, Table S7). Unfortunately, due to small sample size, one-way ANOVA did not

203 indicate statistical significance ($p > 0.05$) (Fig 4C) between these different MoA but did indicate that

204 their longer lag phases resulted in higher BRRoK^{48h} PC1 scores (Figure 4C).

Discussion

The next-generation antimalarial drugs should rapidly eliminate parasite burden, ideally as fast as artesunate, but at least as fast as chloroquine.[1] Whilst we have previously used the BRRoK[6h] assay to measure the relative RoK for 370 Malaria Box compounds, here we show that BRRoK[6h] data provides links to the antimalarial MoA (with PfATP4 > parasite hemoglobin catabolism > DHFR-TS > DHODH > bc1 complex) and that comparison with scaffold sub-structures identified five core scaffolds with the relative RoK: diamino-glycerols > 2-(aminomethyl)phenol > 2-phenylbenzimidazole > 8-hydroxyquinolines > triazolopyrimidine. We also predicted that compounds with minimal activity at 6h might have a lag phase, like atovaquone and DSM265.[7,10,35] Thus, we determined the RoK of apparently slow-acting compounds using a BRRoK[48h] assay and show that many of the slow-acting compounds are likely DHODH and bc_1 complex inhibitors. In short, compounds in the Malaria Box with similar targets and chemical core substructure exhibit similar time-dependant RoK dynamics. Although our study is limited to a library of 400 compounds that lack a full biochemical target validation, it provides the proof-of-principle that BRRoK data offers an opportunity to rapidly prioritize compounds in the TCAMS, or other, library by informing predictions of structure-activity and MoA. Moreover, we note that using the BRRoK assay at two-time points, 6 and 48h, we not only have the potential to rapidly identify and discriminate between compounds that meet the ideal and minimum TCP1 criteria, but also identify compounds that likely exhibit a lag time in drug action between 6 and 48h. This BRRoK assay format, however, does not provide a reliable assessment of the extent and timing of this lag time, as would be reported by a recrudescence assay.[10]

A compound's immediate cytocidal activity likely results from the nature of the target and the ease of access to the target. The first aspect considers how quickly a deficit in this target's function will lead to cell death – i.e. its MoA. In $vitro$ assays of RoK report that antimalarial drugs with a similar MoA result in similar RoK.[7,10] We have significantly extended this observation here for the open Source Malaria Box, a critical collection of antimalarial drug discovery compounds. Whilst

231 an important caveat is that for most compounds described the target association is tentative, this

232 library is still the best described and investigated resource in this endevour.[21] Nonetheless, here we

233 were able to consider five MoA groups due to availability of *in vitro* PRR data and at least 10 MMV

234 compounds annotated for each MoA from a range of sources.[16,20,21,27,28,35] Specifically; **(i) PfATP4**

235 (Figure 1A): 33 compounds are annotated as *Pf*ATP4 inhibitors (Figure 1A).[20,29] *In vitro* PRR data are

236 available for exemplar *Pf*ATP4 inhibitors (+)-SJ733,36[21] a dihydroisoquinoline with a slow-to-

237 moderate RoK, and KAE609/NITD609,[27] a spiroindolone with a moderate to fast RoK. Most potential

238 Malaria Box *Pf*ATP4 inhibitors were reported as having a BRRoK[6h] between the moderate mefloquine

239 [10] (comparable to the PRR reference pyrimethamine[10]) and the rapidly-acting dihydroartemisinin.

240 The fastest-acting *Pf*ATP4 inhibitor was the spiroindolone MMV396749, with several studies

241 reporting a fast to moderate cytocidal activity for *Pf*ATP4 inhibitors.[7,16,20,21,27,29] The Malaria Box also

242 contains five structural analogues of the slower acting *Pf*ATP4 inhibitor (+)-SJ733; two have PC1s

243 falling between the fast-acting dihydroartemisinin and chloroquine with the remaining three

244 between mefloquine and atovaquone, supporting the prediction of a moderate to slow RoK of the

245 dihydroisoquinolines. **(ii) *Plasmodium* dihydrofolate reductase-thymidylate synthase (DHFR-TS)**

246 (Figure 1B): 14 compounds are annotated as DHFR-TS inhibitors, clustering with known antifolate

247 antimalarial drugs that target DHFR-TS, P218, pyrimethamine, and WR99210.[29,40–42] Pyrimethamine

248 has a lag phase of 24 h, which is the slowest RoK after ATQ.[10] The BRRoK[6h] confirms slow cytocidal

249 activity for this cluster, between slow-acting atovaquone and moderate-acting pyronaridine. **(iii)**

250 **Dihydroorotate dehydrogenase (DHODH)** (Figure 1C): 43 compounds are annotated as DHODH

251 inhibitors, and BRRoK[6h] show that they share a slow initial cytocidal action. This slow RoK correlates

252 with the atovaquone-like *in vitro* PRR data for DSM265[35], due to its 24-48h lag phase. One outlier,

253 MMV666102, falls between pyronaridine and mefloquine showing a slow-to-moderate cytocidal

254 action. Whilst no additional target information is available, we predict that this compound may have

255 additional targets. **(iv) bc$_1$ complex inhibitors:** 18 compounds are annotated as bc$_1$ complex

256 inhibitors and are slowly cytocidal in the BRRoK[6h] and are comparable to atovaquone which shares

257   the same MoA.[10] Comparing BRRoK with the predicted MoA for all four groups indicates that

258   compounds with a similar MoA have similar RoK. The predicted MoA used here was primarily

259   obtained through metabolomics[16,29,30] and readily highlights the potential for BRRoK to complement

260   such studies. **(v) Parasite hemoglobin catabolism:** Allman *et al.,*[29] reports a compound group in the

261   Malaria Box that perturbs parasite hemoglobin catabolism. Parasite hemoglobin catabolism

262   compounds formed our second fastest-acting cluster (Figure 1E). However, as expected, the BRRoK[6h]

263   data reveals a broad RoK range for these compounds, which agrees with metabolomics data, as

264   these compounds have a range of predicted targets. For example, chloroquine, known for

265   accumulation within the digestive vacuole of *Plasmodium,* clusters with this group, but the resulting

266   metaprint is divergent, due to the overall lack of significant metabolic changes or dysregulation

267   induced by chloroquine.[29,43] MMV390048, which inhibits the phosphatidylinositol 4-kinase (PI4K),

268   and AZ412, which inhibits the putative vacuolar ATPase,[12,29,44] also clusters with this group.

269   Interestingly, as expected from compounds with different targets, the BRRoK[6h] appears to form

270   subclusters within this group. Upon additional target data availability, we would predict that this

271   currently broad class of compounds could be further categorised into slow, moderate, and fast-

272   acting groups.

273   A second means to classify compounds for comparison to the BRRoK[6hr] data is through their

274   chemical structure (Figure 2). Our analysis suggests that structurally similar compounds exert a

275   similar RoK. This is not surprising if they share the same target, and our analysis suggests that

276   medicinal chemistry may not only improve IC$_{50}$ potency for candidates but may also help improve

277   RoK within chemical class and a well-defined MoA. For example, all five triazolopyrimidine scaffold

278   members (Figure 2A) inhibit DHODH and are structural analogs of DSM265, a known slow-acting

279   compound in clinical trials.[35] However, their PC1 varies between 23 and 67, highlighting room to

280   influence the initial cytocidal action within the limits of this chemical class and the intrinsic limits of

281   the MoA. A range of slow cytocidal activity is also reported for 8-hydroxyquinolines (PC1 of 8.8-95.4)

282   (Figure 2B), with one annotated as a DHODH inhibitor. We also report two fast-acting scaffolds:

283   diamino-glycerols and 2-(aminomethyl)phenol (Figure 2C-D).   The diamino-glycerol is the fastest

284   scaffold described here, which agrees with a predicted MoA as four of these nine compounds are

285   *Pf*ATP4 inhibitors.[16,20,29] It would be interesting to investigate whether the remaining five compounds

286   also affect *Pf*ATP4. Three of these five compounds are designated as probe-like and were not

287   characterised in metabolomic studies that focussed on drug-like compounds in the Malaria Box.[29]

288   Furthermore, five compounds are structurally related to the amino alcohol-carbazoles, which has

289   demonstrated long-lasting and fast-acting antimalarial activity *in vivo*,[45] in agreement with BRRoK[6h]

290   measurements here. The next most fast-acting compound cluster is the 2-(aminomethyl)phenol

291   scaffold. Interestingly, BRRoK[6h] indicated five of 14 compounds in this scaffold are likely inhibitors of

292   parasite hemoglobin catabolism (PC1 between -79 and -51),[29] which is the second fastest-acting

293   compound cluster according to MoA comparisons and agrees with our chemical clustering analyses.

294   Eight compounds are probe-like, so metabolomic data are not available, however, Creek *et al.*[43] have

295   shown an artemisinin-like metabolomic signature for three of these compounds, thus confirming the

296   relative fast action of this scaffold. These data illustrate how BRRoK data can be effectively

297   employed alongside other datasets to inform how decisions are made regarding the selection of

298   targets for further study and/or development.

299   Given the short timeframe of the BRRoK[6h], a second attribute that may influence RoK is ease

300   of target access**.** Within our *in vitro* assay, compounds must migrate through up to four membranes

301   to access a target within an infected erythrocyte and the biophysical parameters of size,

302   hydrophobicity, hydrogen-bonding capabilities and charge may contribute to how easily access

303   occurs. Another consideration for compounds with a basic charge at physiological pH, is that of

304   access/accumulation within the digestive vacuole in the trophozoite, irrespective of the final target

305   site. Biophysical properties span charge type, lipophilicity, polarity, size, 3D-shape, flexibility and H-

306   bond properties.[46] To investigate what influence molecular properties have on BRRoK[6h], we

307   calculated key biophysical properties for Malaria Box compounds (PC1) (Table S8) and compared

308   compounds with relative RoK faster than DHA and slower than atovaquone to see if extremes of RoK

309 are associated with significantly different molecular properties. We expanded analyses to include

310 compounds reported to have a common, fast MoA (PfATP4), a common, slow MoA (bc$_1$ complex), a

311 common fast core (2-(Methylamino)-Phenols, 2-MAP), and a common, slow core (2-

312 Phenylbenzimidazoles, 2-Ph-Bz) (Table S8-9). These analyses do not reveal molecular property

313 differences associated with BRRoK, although an important limitation here are the numbers of

314 compounds in each group. Finally, we compared individual compounds with the fastest BRRoK^{6h} and

315 slowest BRRoK^{6h} in the five MoA clusters investigated here and found some small differences (Table

316 S10). The fastest compound in each MoA often has a lower MW, less rotatable bonds and is more

317 aromatic in nature compared to the slowest, suggesting that careful biophysical property control

318 may allow compound design to achieve improvements in RoK within a well-defined MoA/chemical

319 class.

320 Perhaps the key benefit of RoK analysis considering both the MoA and chemical substructure

321 is that outliers emerge that would appear to warrant additional validation or follow up. An example

322 from this study are the three 1,2-diaza-9-fluorenones (MMV666021, MMV6666026 and

323 MMV665934) for which the proposed MoA is the bc$_1$ complex, which would imply a very slow RoK.

324 However, we instead found that two of these have very fast BRRoK. Also, of interest is the structural

325 singleton MMV142383, which has the fastest RoK (PC1= -131.5) and is categorised as acting by

326 hemoglobin catabolism. Exceptions found using sub-structure analysis may have either

327 miscategorized MoA or alternatively, they may have more than one MoA. The latter would be of

328 particular interest as would theoretically lead to less resistance if more than one target is involved.

329 In summary, we provide a demonstration that for leading antimalarial drug discovery

330 compounds that their RoK are related to their MoA, and that a compound's RoK is also likely

331 modified by factors that affect target access. Thus, as we use medicinal chemistry to improve

332 compound potency, we could also influence the RoK for some scaffolds. Our modified BRRoK assay

333 provides the necessary throughput for drug discovery and a critical decision-making tool to support

334 development campaigns. Although our study was performed on a small pool of compounds, the

335 scaffolds we identified provide a strong basis for discovery antimalarial prioritization. Our core

336 analysis approach has identified two scaffolds, diamino-glycerols, and 2-(aminomethyl) phenol, that

337 exhibit fast cytocidal action, inviting medicinal chemistry improvements towards possible TCP1

338 candidates. Some less-represented scaffolds have also been identified with fast cytocidal action, and

339 medicinal chemistry may allow discovery of compounds that meet the TCP1 profile. Further insights

340 might be gained from our data, as targets are defined for additional MMV compounds.

341

354

355   **Transparency declarations**

356   None to declare.

357

358   **Supplementary data**

359   Supplementary Figures S1 to S4 and Tables S1 to S10 are available at JAC Online (http://jac.oxford

360   journals.org/).

361

362   **References**

363   1.   Burrows JN, Hooft Van Huijsduijnen R, Möhrle JJ, *et al.* Designing the next generation of

364   medicines for malaria control and eradication. *Malar J* 2013; **12** : 187.

365   2.   Spangenberg T, Burrows JN, Kowalczyk P, *et al.* The open access Malaria Box: A drug

366   discovery catalyst for neglected diseases. *PLoS One* 2013; **8** : e62926.

367   3.   Gamo F-J, Sanz LM, Vidal J, *et al.* Thousands of chemical starting points for antimalarial lead

368   identification. *Nature* 2010; **465** : 305–310.

369   4.   Guiguemde WA, Shelat AA, Bouck D, *et al.* Chemical genetics of Plasmodium falciparum.

370   *Nature* 2010; **465** : 311–315.

371   5.   Plouffe D, Brinker A, McNamara C, *et al.* In silico activity profiling reveals the mechanism of

372   action of antimalarials discovered in a high-throughput screen. *Proc Natl Acad Sci* 2008; **105** :

373   9059–9064.

374   6.   Meister S, Plouffe DM, Kuhen KL, *et al.* Imaging of *Plasmodium* liver stages to drive next-

375   generation antimalarial drug discovery. *Science (80-)* 2011; **334** : 1372–1377.

376   7.   Ullah I, Sharma R, Biagini GA, *et al.* A validated bioluminescence-based assay for the rapid

377   determination of the initial rate of kill for discovery antimalarials. *J Antimicrob Chemother*

378   2017; **72** : 717–726.

379   8.   Burrows JN, Duparc S, Gutteridge WE, *et al.* New developments in anti-malarial target

380   candidate and product profiles. *Malaria Journal* 2017; **16** : 26.

381   9.   White NJ. Assessment of the pharmacodynamic properties of antimalarial drugs *in vivo*.

382   *Antimicrobial Agents and Chemotherapy* 1997; **41** : 1413–1422.

383   10.   Sanz LM, Crespo B, De-Cózar C, *et al. P. falciparum in vitro* killing rates allow to discriminate

384   between different antimalarial mode-of-action. *PLoS One* 2012; **7** : e30949.

385   11.   Baragaña B, Hallyburton I, Lee MCS, *et al.* A novel multiple-stage antimalarial agent that

386   inhibits protein synthesis. *Nature* 2015; **522** : 315–320.

387   12.   Hameed P. S, Solapure S, Patil V, *et al.* Triaminopyrimidine is a fast-killing and long-acting

388   antimalarial clinical candidate. *Nat Commun* 2015; **6** : 6715.

389   13.   McConville M, Fernández J, Angulo-Barturen Í, *et al.* Carbamoyl triazoles, known serine

390   protease inhibitors, are a potent new class of antimalarials. *J Med Chem* 2015; **58** : 6448–

391   6455.

392   14.   Wong EH, Hasenkamp S & Horrocks P. Analysis of the molecular mechanisms governing the

393   stage-specific expression of a prototypical housekeeping gene during intraerythrocytic

394   development of *P. falciparum*. *J Mol Biol* 2011; **408** : 205–221.

395 15. Hasenkamp S, Sidaway A, Devine O, *et al.* Evaluation of bioluminescence-based assays of anti-

396   malarial drug activity. *Malar J* 2013; **12** : 58.

397 16. Van Voorhis WC, Adams JH, Adelfio R, *et al.* Open source drug discovery with the Malaria Box

398   compound collection for neglected diseases and beyond. *PLoS Pathog* 2016; **12** : e1005763.

399 17. Hasenkamp S, Wong EH & Horrocks P. An improved single-step lysis protocol to measure

400   luciferase bioluminescence in *Plasmodium falciparum*. *Malar J* 2012; **11** : 42.

401 18. Zhang J-H, Chung TDY & Oldenburg KR. A simple statistical parameter for use in evaluation

402   and validation of high throughput screening assays. *J Biomol Screen* 1999; **4** : 67–73.

403 19. Berthold MR, Cebron N, Dill F, *et al.* KNIME - the Konstanz information miner. In: Preisach

404   CBerhardt HSchmidt-Theime Let al. ., eds. Data Analysis,. *Mach Learn Appl Ger Springer* 2009;

405   **11** : 26.

406 20. Lehane AM, Ridgway MC, Baker E, *et al.* Diverse chemotypes disrupt ion homeostasis in the

407   malaria parasite. *Mol Microbiol* 2014; **94** : 327–339.

408 21. Fedewa G, Clark JA, Kirk K, *et al.* (+)-SJ733, a clinical candidate for malaria that acts through

409   ATP4 to induce rapid host-mediated clearance of Plasmodium. *Proc Natl Acad Sci* 2014; **111** :

410   E5455-62.

411 22. Fong KY, Sandlin RD & Wright DW. Identification of β-hematin inhibitors in the MMV Malaria

412   Box. *Int J Parasitol Drugs Drug Resist* 2015; **5** : 84–91.

413 23. Liu L, Richard J, Kim S, *et al.* Small molecule screen for candidate antimalarials targeting

414   *Plasmodium Kinesin-5*. *J Biol Chem* 2014; **289** : 16601–16614.

415 24. Dickerman BK, Elsworth B, Cobbold SA, *et al.* Identification of inhibitors that dually target the

416   new permeability pathway and dihydroorotate dehydrogenase in the blood stage of

417   *Plasmodium falciparum*. *Sci Rep* 2016; **6** : 37502.

418 25. Tiwari NK, Reynolds PJ & Calderón AI. Preliminary LC-MS Based Screening for Inhibitors of

419   *Plasmodium falciparum* Thioredoxin Reductase (*Pf*TrxR) among a Set of Antimalarials from

420   the Malaria Box. *Molecules* 2016; **21** : 424.

421   26.   Paiardini A, Bamert RS, Kannan-Sivaraman K, *et al.* Screening the medicines for malaria

422   venture 'Malaria Box' against the *Plasmodium falciparum* Aminopeptidases, M1, M17 and

423   M18. *PLoS One* 2015; **10** : e0115859.

424   27.   Rottmann M, McNamara C, Yeung BKS, *et al.* Spiroindolones, a potent compound class for the

425   treatment of malaria. *Science (80-)* 2010; **329** : 1175–1180.

426   28.   Coteron JM, Marco M, Esquivias J, *et al.* Structure-guided lead optimization of

427   triazolopyrimidine-ring substituents identifies potent *Plasmodium falciparum* dihydroorotate

428   dehydrogenase inhibitors with clinical candidate potential. *J Med Chem* 2011; **54** : 5540–61.

429   29.   Allman EL, Painter HJ, Samra J, *et al.* Metabolomic profiling of the malaria box reveals

430   antimalarial target pathways. *Antimicrob Agents Chemother* 2016; **60** : 6635–6649.

431   30.   Creek DJ, Chua HH, Cobbold SA, *et al.* Metabolomics-based screening of the Malaria Box

432   reveals both novel and established mechanisms of action. *Antimicrob Agents Chemother*

433   2016; **60** : 6650–6663.

434   31.   Bahamontes-Rosa N, Rodríguez-Alejandre A, González-Del-Rio R, *et al.* A new molecular

435   approach for cidal vs static antimalarial determination by quantifying mRNA levels. *Mol*

436   *Biochem Parasitol* 2012; **181** : 171–177.

437   32.   Linares M, Viera S, Crespo B, *et al.* Identifying rapidly parasiticidal anti-malarial drugs using a

438   simple and reliable *in vitro* parasite viability fast assay. *Malar J* 2015; **14** : 441.

439   33.   Pukrittayakamee S, Chantra A, Simpson JA, *et al.* Therapeutic responses to different

440   antimalarial drugs in *vivax* malaria. *Antimicrob Agents Chemother* 2000; **44** : 1680–1685.

441   34.   Ahyong V, Sheridan CM, Leon KE, *et al.* Identification of *Plasmodium falciparum* specific

442   translation inhibitors from the MMV Malaria Box using a high throughput *in vitro* translation

443   screen. *Malar J* 2016; **15** : 173.

444   35.   Phillips MA, Lotharius J, Marsh K, *et al.* A long-duration dihydroorotate dehydrogenase

445   inhibitor (DSM265) for prevention and treatment of malaria. *Sci Transl Med* 2015; **7** :

446   296ra111.

447   36.   Aroonsri A, Akinola O, Posayapisit N, *et al.* Identifying antimalarial compounds targeting

448   dihydrofolate reductase-thymidylate synthase (DHFR-TS) by chemogenomic profiling. *Int J*

449   *Parasitol* 2016; **46** : 527–35.

450   37.   Von Koschitzky I, Gerhardt H, Lämmerhofer M, *et al.* New insights into novel inhibitors

451   against deoxyhypusine hydroxylase from *Plasmodium falciparum*: Compounds with an iron

452   chelating potential. *Amino Acids* 2015; **47** : 1155–66.

453   38.   Hain AUP, Bartee D, Sanders NG, *et al.* Identification of an Atg8-Atg3 protein-protein

454   interaction inhibitor from the medicines for malaria venture malaria box active in blood and

455   liver stage *Plasmodium falciparum* parasites. *J Med Chem* 2014; **57** : 4521–4531.

456   39.   Vallières C & Avery S V. The candidate antimalarial drug mmv665909 causes oxygen-

457   dependent mrna mistranslation and synergizes with quinoline-derived antimalarials.

458   *Antimicrob Agents Chemother* 2017; **61** : e00459-17.

459   40.   Basco LK, de Pécoulas PE, Wilson CM, *et al.* Point mutations in the dihydrofolate reductase-

460   thymidylate synthase gene and pyrimethamine and cycloguanil resistance in *Plasmodium*

461   *falciparum*. *Mol Biochem Parasitol* 1995; **69** : 135–138.

462   41.   Canfield CJ, Milhous WK, Ager AL, *et al.* PS-15: a potent, orally active antimalarial from a new

463   class of folic acid antagonists. *Am J Trop Med Hyg* 1993; **49** : 121–6.

464   42.   Yuthavong Y, Tarnchompoo B, Vilaivan T, *et al.* Malarial dihydrofolate reductase as a

465   paradigm for drug development against a resistance-compromised target. *Proc Natl Acad Sci*

466   *U S A* 2012; **109** : 16823–8.

467   43.   Cobbold SA, Chua HH, Nijagal B, *et al.* Metabolic dysregulation induced in *Plasmodium*

468   *falciparum* by dihydroartemisinin and other front-line antimalarial drugs. *J Infect Dis* 2016;

469   **213** : 276–286.

470   44.   Younis Y, Douelle F, Feng T-S, *et al.* 3,5-Diaryl-2-aminopyridines as a novel class of orally

471   active antimalarials demonstrating single dose cure in mice and clinical candidate potential. *J*

472   *Med Chem* 2012; **55** : 3479–3487.

473   45.   Charman SA, Greco B, Bashyam S, *et al.* Long-lasting and fast-acting *in vivo* efficacious

474   antiplasmodial azepanylcarbazole amino alcohol. *ACS Med Chem Lett* 2017; **8** : 1304–1308.

475   46.   Veber DF, Johnson SR, Cheng HY, *et al.* Molecular properties that influence the oral

476   bioavailability of drug candidates. *J Med Chem* 2002; **45** : 2615–23.

477

479
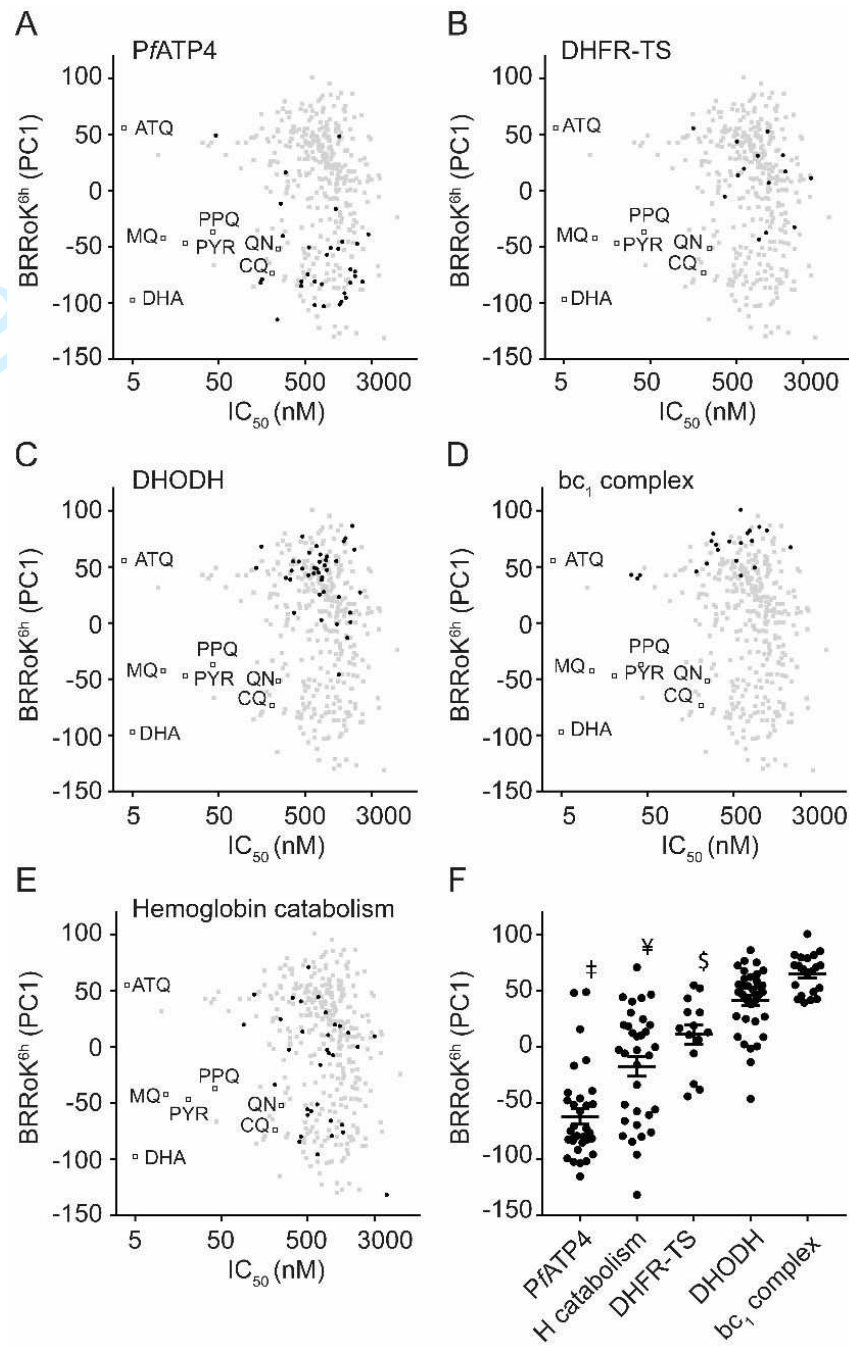
Figure 1. **Correlating mode of drug action with the BRRoK^{6h} in the MMV Malaria Box compounds.**

Zero-meaned PC1 data for known antimalarial drugs (open squares), all Malaria Box compounds (grey filled squares) and Malaria Box compounds predicted to use the indicated MoA (black filled circles) for (**A**) PfATP4, (**B**) parasite hemoglobin catabolism, (**C**) dihydrofolate reductase-thymidylate synthase (DHFR-TS), (**D**), dihydroorotate dehydrogenase (DHODH) and (**E**) mitochrondrial bc_1 complex are plotted against their IC$_{50}$. Faster initial rates of cytocidal activity are represented with

486   lower PC1 values. See Table S2 for PC1, IC_{50} and predicted MoA data for individual compounds. (**F**)

487   One-way ANOVA with post-hoc Tukey test comparing the BRRoK[6h] data[7] for each MoA group

488   (whisker plots represent the mean and SD)[16,20,29,30]. **‡** = *Pf*ATP4 cluster, significantly different from all

489   clusters ($p < 0.01$). **¥** = parasite hemoglobin catabolism (H catabolism), significantly different than

490   DHODH and bc_1 complex ($p < 0.01$). **$** = DHFR-TS, significantly different than the bc_1 complex ($p <$

491   0.01). ATQ, atovaquone; CQ, chloroquine; DHA, dihydroartemisinin; MQ, mefloquine; PPQ,

492   piperaquine; PYN, pyronaridine; QN, quinine.

494

495
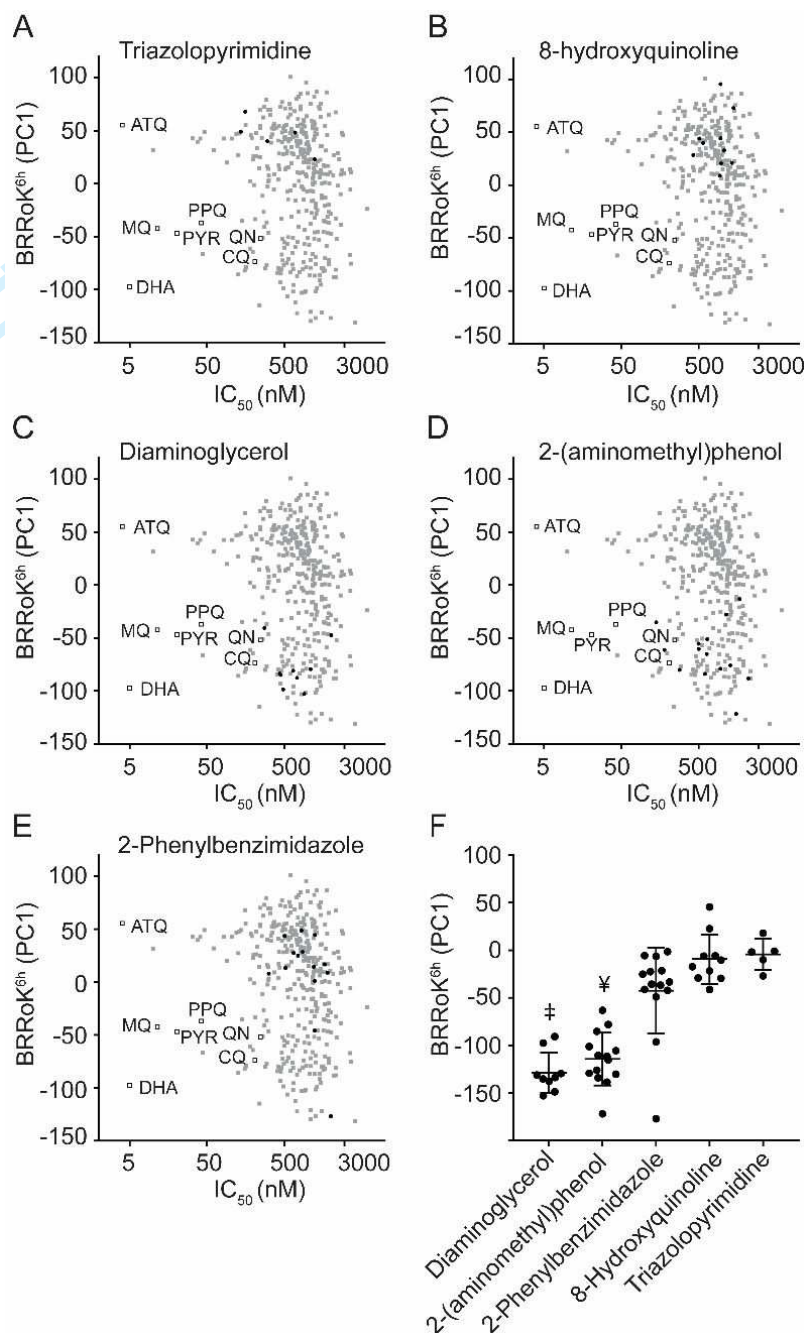
Figure 2. BRRoK^{6h} data illustrates related compounds in the MMV Malaria Box that share a similar relative RoK. Zero-meaned PC1 data for known antimalarial drugs (open squares), all Malaria Box compounds (grey filled squares) and Malaria Box compounds sharing the indicated related core scaffolds (black filled circles) of (**A**) diamino-glycerols, (**B**) 2-(aminomethyl)phenol, (**C**) 2-phenylbenzimidazole, (**D**) 8-hydroxyquinolines, and (**E**) triazolopyrimidine are plotted against their

501   IC_{50}. Faster initial rates of cytocidal activity are represented with lower PC1 values. See Table S3 for

502   PC1, IC_{50} and structures for individual compounds. (**F**) One-way ANOVA with post-hoc Tukey test

503   comparing the BRRoK[6h] data[7] for each group (whisker plots represent the mean and SD) based on

504   the indicted related core scaffold. ‡ = Diamino-glycerols, significantly different than 2-

505   phenylbenzimidazole, 8-hydroxyquinolines, and triazolopyrimidine scaffolds ($p < 0.01$). **$** = 2-

506   (aminomethyl)phenol, significantly different than 2-phenylbenzimidazole, 8-hydroxyquinolines, and

507   triazolopyrimidine scaffolds ($p < 0.01$). ATQ, atovaquone; CQ, chloroquine; DHA, dihydroartemisinin;

508   MQ, mefloquine; PPQ, piperaquine; PYN, pyronaridine; QN, quinine.

510

511
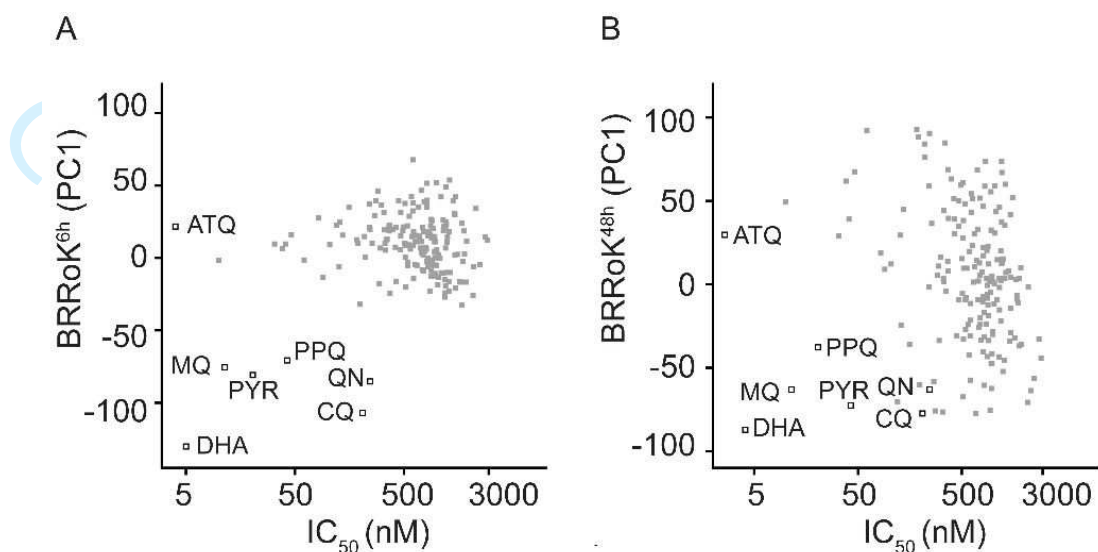
Figure 3. Distribution of BRRoK (PC1) against IC$_{50}$ for the MMV Malaria Box compounds.

Zero-meaned PC1 data for 178 compounds in the MMV Malaria Box (grey filled squares) and 7

benchmark antimalarial drugs (open squares) are plotted against their IC$_{50}$ for (**A**) 6hr and (**B**) 48h.

See Table S2 for PC1 and IC$_{50}$ data for individual compounds. ATQ, atovaquone; CQ, chloroquine;

DHA, dihydroartemisinin; MQ, mefloquine; PPQ, piperaquine; PYN, pyronaridine; QN, quinine.

518

519
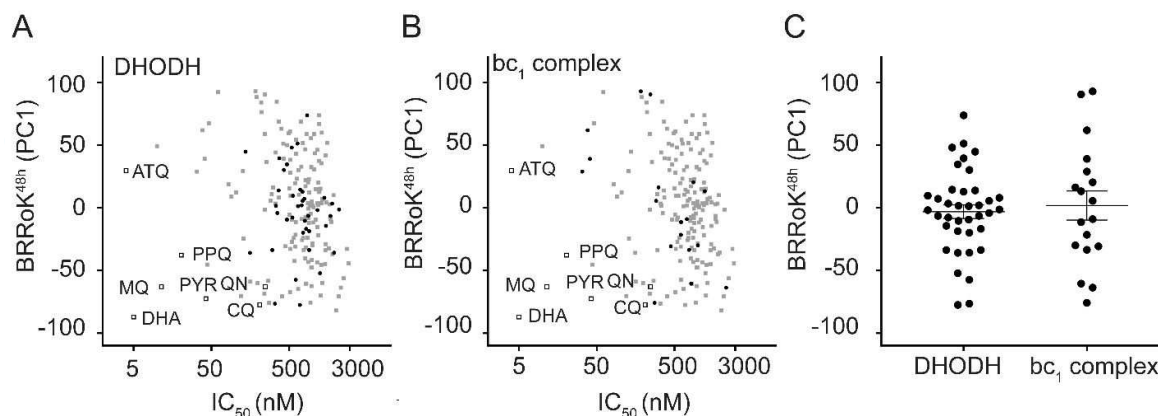
Figure 4. **Correlating mode of drug action with the BRRoK[48h] in the MMV Malaria Box compounds**.

Zero-meaned PC1 data for known antimalarial drugs (open squares), all Malaria Box compounds

(grey filled squares) and Malaria Box compounds with a predicted MoA (black filled circles) that

targets, (**A**) DHODH or (**B**) the bc1 complex are plotted against their IC_{50}. See Table S2 for PC1,

IC_{50} and predicted MoA data for individual compounds. (**C**) One-way ANOVA with post-hoc Tukey

test comparing the BRRoK[48h] data (whisker plots represent the mean and SD) for both groups

clustered based on the indicted predicted MoA data[16,20,29,30]. No significant difference was found (p =

0.6). ATQ, atovaquone; CQ, chloroquine; DHA, dihydroartemisinin; MQ, mefloquine; PPQ,

piperaquine; PYN, pyronaridine; QN, quinine.

529

Supplementary data

The relative rate of kill of the MMV Malaria Box compounds provide links

to the mode of antimalarial action and highlight scaffolds of medicinal

chemistry interest

Imran ULLAH^1, Raman SHARMA[2], Antonio METE[3], Giancarlo A. BIAGINI[2], Dawn M. WETZEL[4]

and Paul D. HORROCKS*[1]

[1]Institute for Science and Technology in Medicine, Keele University, Staffordshire ST5 5BG,

United Kingdom; [2]Research Centre for Drugs and Diagnostics, Liverpool School of Tropical Medicine,

Pembroke Place, Liverpool L3 5QA, United Kingdom; [3]Medsyndesign Ltd, Advanced Technology

Innovation Centre, 5 Oakwood Drive, Loughborough, LE11 3QF, United Kingdom; [4]Department of

Pediatrics, University of Texas Southwestern Medical Center, Dallas, 75235 Texas, USA

*Corresponding author. Institute for Science and Technology in Medicine, Keele University, Staffordshire

ST5 5BG, United Kingdom.

Tel: +44-(0)-1782-733670

E-mail: p.d.horrocks@keele.ac.uk

Running title: Antimalarial relative rate of kill

Table S1: The antimalarial drugs were sourced from Sigma–Aldrich and prepared as shown below and were stored at −20 °C. The Malaria Box was provided by MMV (www.mmv.org) and was provided as 20 µL solutions of 10 mM concentration in DMSO and stored at −20 °C.

Drug/compound	Stock Concentration	Solvent
Atovaquone (AQ)	10mM	DMSO
Artemether	50mM	Ethanol
Chloroquine	100mM	Deionized water
Dihydroartemisinin	50 mM	Methanol
Mefloquine	50 mM	DMSO
Piperaquine	100mM	Ethanol
Pyronaridine	100mM	Deionized water
Quinine	50mM	Ethanol
Malaria Box compounds	10mM	DMSO
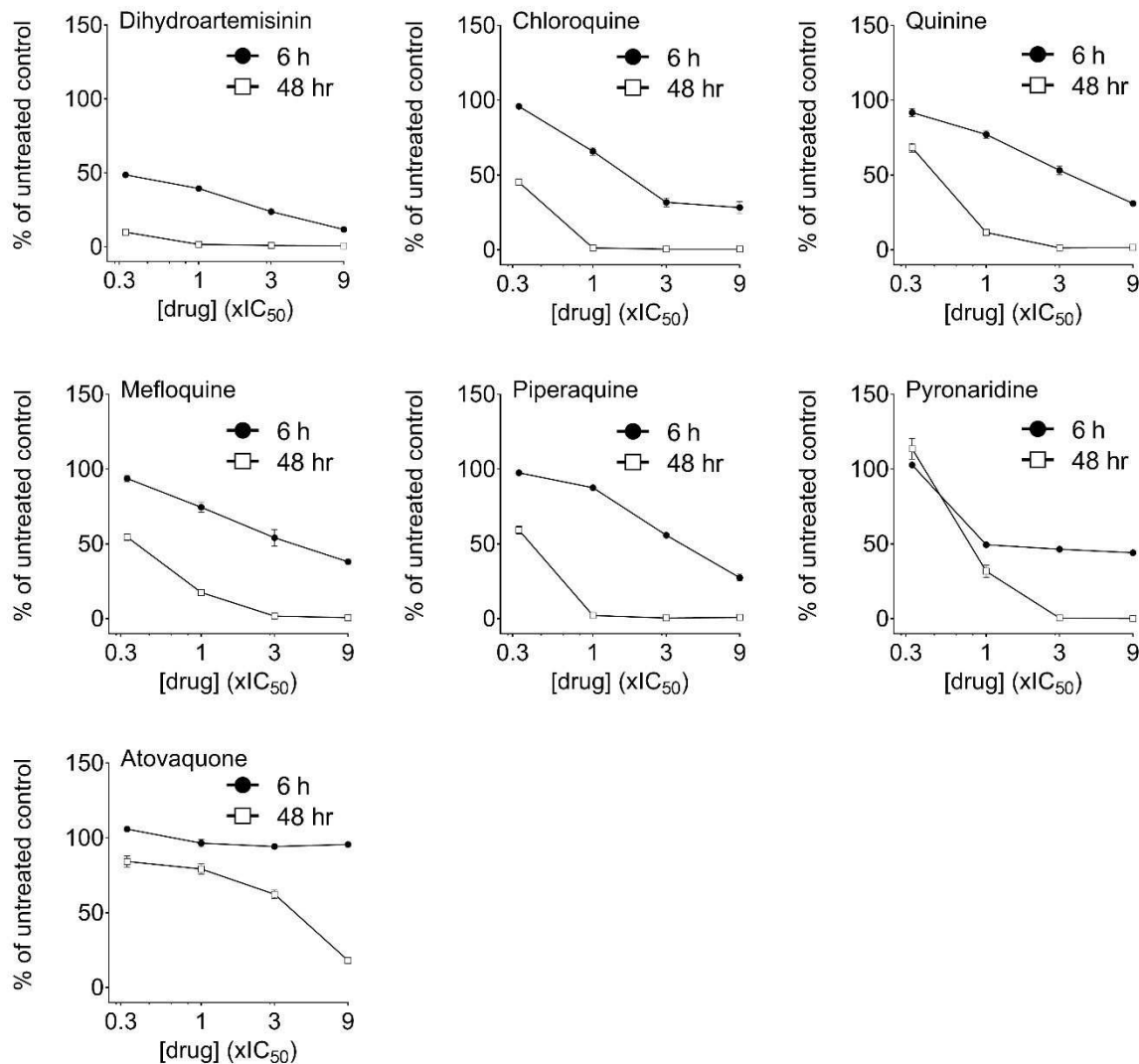
Figure S1: Equipotent IC$_{50}$ concentration-dependent loss of bioluminescence for standard antimalarial drugs. The mean (error bars represent ±SD from three biological replicates) bioluminescence signal, normalized against an untreated control, remaining after a 6 (closed circles) or 48 h (open squares) exposure to the indicated fold-IC$_{50}$ concentration of drug. A serial 3-fold dilution from 9 × IC$_{50}$ to 0.33 × IC$_{50}$ is reported. See Figure S1 and S2 for 178 compounds of the MMV Malaria Box compounds.

Table S4 is to be used in conjunction with panels (drug-like) D1 to D11 and (probe-like) P1 to P10 in Figures S2 and S3, respectively. Listed below are the Compound ID for the MMV Malaria Box compounds tested in this study. The panel on which the dose-response curve for that compound is shown in these supplementary materials is indicated below.

COMPOUND_ID Drug-Like	Position	COMPOUND_ID Probe-Like	Position
MMV019066	D1	MMV396680	P1
MMV011259	D1	MMV666601	P1
MMV006278	D1	MMV008294	P1
MMV006427	D1	MMV666688	P1
MMV020439	D1	MMV666062	P1
MMV396672	D1	MMV020885	P1
MMV019871	D1	MMV008416	P1
MMV665874	D1	MMV665977	P1
MMV001246	D1	MMV666607	P1
MMV665916	D2	MMV007695	P2
MMV011099	D2	MMV666101	P2
MMV020492	D2	MMV666596	P2
MMV665782	D2	MMV396679	P2
MMV665876	D2	MMV666691	P2
MMV396703	D2	MMV000642	P2
MMV006937	D2	MMV666600	P2
MMV665820	D2	MMV006309	P2
MMV007116	D2	MMV666023	P2
MMV020548	D3	MMV007160	P3
MMV019258	D3	MMV085203	P3
MMV011256	D3	MMV007384	P3
MMV666693	D3	MMV665827	P3
MMV008956	D3	MMV396678	P3
MMV007839	D3	MMV006861	P3
MMV000662	D3	MMV006457	P3
MMV666103	D3	MMV396693	P3
MMV666057	D3	MMV665908	P3
MMV007564	D4	MMV666054	P4
MMV000563	D4	MMV007127	P4
MMV665850	D4	MMV006389	P4
MMV666105	D4	MMV665934	P4
MMV666072	D4	MMV665994	P4
MMV665909	D4	MMV665980	P4
MMV665940	D4	MMV007577	P4
MMV665899	D4	MMV000720	P4
MMV665961	D4	MMV006753	P4

MMV666108	D5	MMV666125	P5
MMV006188	D5	MMV007574	P5
MMV665799	D5	MMV007557	P5
MMV008149	D5	MMV000699	P5
MMV019074	D5	MMV009127	P5
MMV665798	D5	MMV006250	P5
MMV666067	D5	MMV007199	P5
MMV665939	D5	MMV085471	P5
MMV009060	D5	MMV665797	P5
MMV019758	D6	MMV666095	P6
MMV665901	D6	MMV019690	P6
MMV666081	D6	MMV019241	P6
MMV666009	D6	MMV665783	P6
MMV019746	D6	MMV000787	P6
MMV666093	D6	MMV666106	P6
MMV007571	D6	MMV666022	P6
MMV665954	D6	MMV498479	P6
MMV666075	D6	MMV007396	P6
MMV666070	D7	MMV665923	P7
MMV000788	D7	MMV007228	P7
MMV665879	D7	MMV073843	P7
MMV006913	D7	MMV667492	P7
MMV008127	D7	MMV007764	P7
MMV403679	D7	MMV665886	P7
MMV019700	D7	MMV396664	P7
MMV019670	D7	MMV086103	P7
MMV001344	D7	MMV084434	P7
MMV019124	D8	MMV666692	P8
MMV006767	D8	MMV665836	P8
MMV007808	D8	MMV665875	P8
MMV396681	D8	MMV396726	P8
MMV019202	D8	MMV006962	P8
MMV075490	D8	MMV396652	P8
MMV007374	D8	MMV008160	P8
MMV020700	D8	MMV665810	P8
MMV007906	D8	MMV665927	P8
MMV000911	D9	MMV009085	P10
MMV007430	D9	MMV638723	P10
MMV007977	D9	MMV396594	P10
MMV665883	D9	MMV396665	P10
MMV084940	D9	MMV396723	P10
MMV000963	D9	MMV011832	P10
MMV006319	D9	MMV665898	P10
MMV000972	D9	MMV665814	P10
MMV665904	D9	MMV007041	P10

|			
MMV006820	D10	MMV645672	P11
MMV011576	D10	MMV011438	P11
MMV020651	D10	MMV665840	P11
MMV396705	D10	MMV667489	P11
MMV007881	D10	MMV396770	P11
MMV008212	D10		
MMV007791	D10		
MMV665843	D10		
MMV396595	D10		
MMV019762	D11		
MMV020942	D11		

Figure S2. Equipotent-IC_{50} concentration-dependent loss of bioluminescence plots for drug-like compounds screened from the MMV Malaria Box. The data for these drug-like compounds are shown on seven panels (**D1-11**). The mean (error bars represent SD from three biological replicates) bioluminescence signal, normalised against an untreated control, remaining after a 6 h (closed circles) or 48 h (open squares) exposure to the indicated fold-IC_{50} concentration of drug.

D1

D2

D3

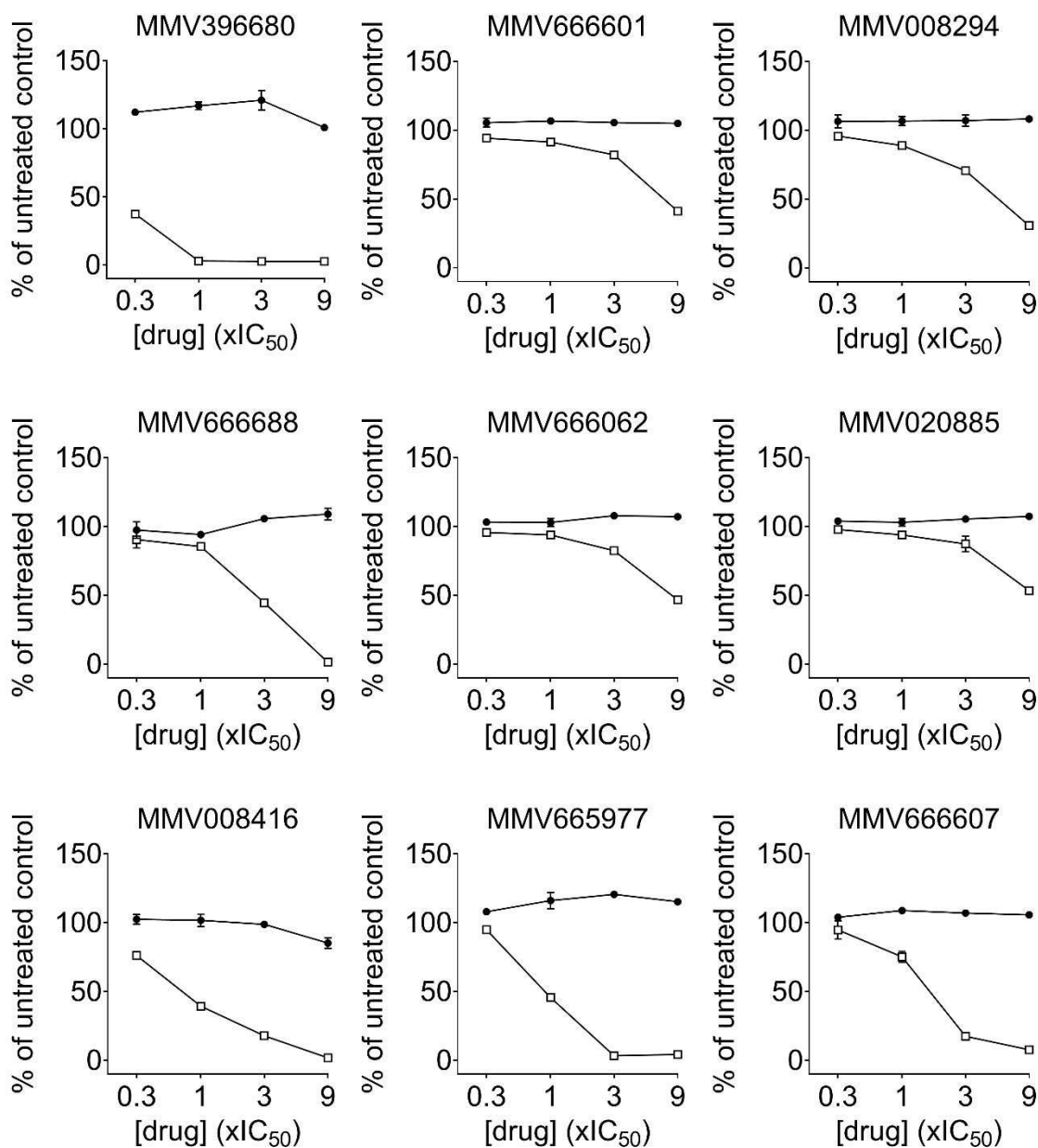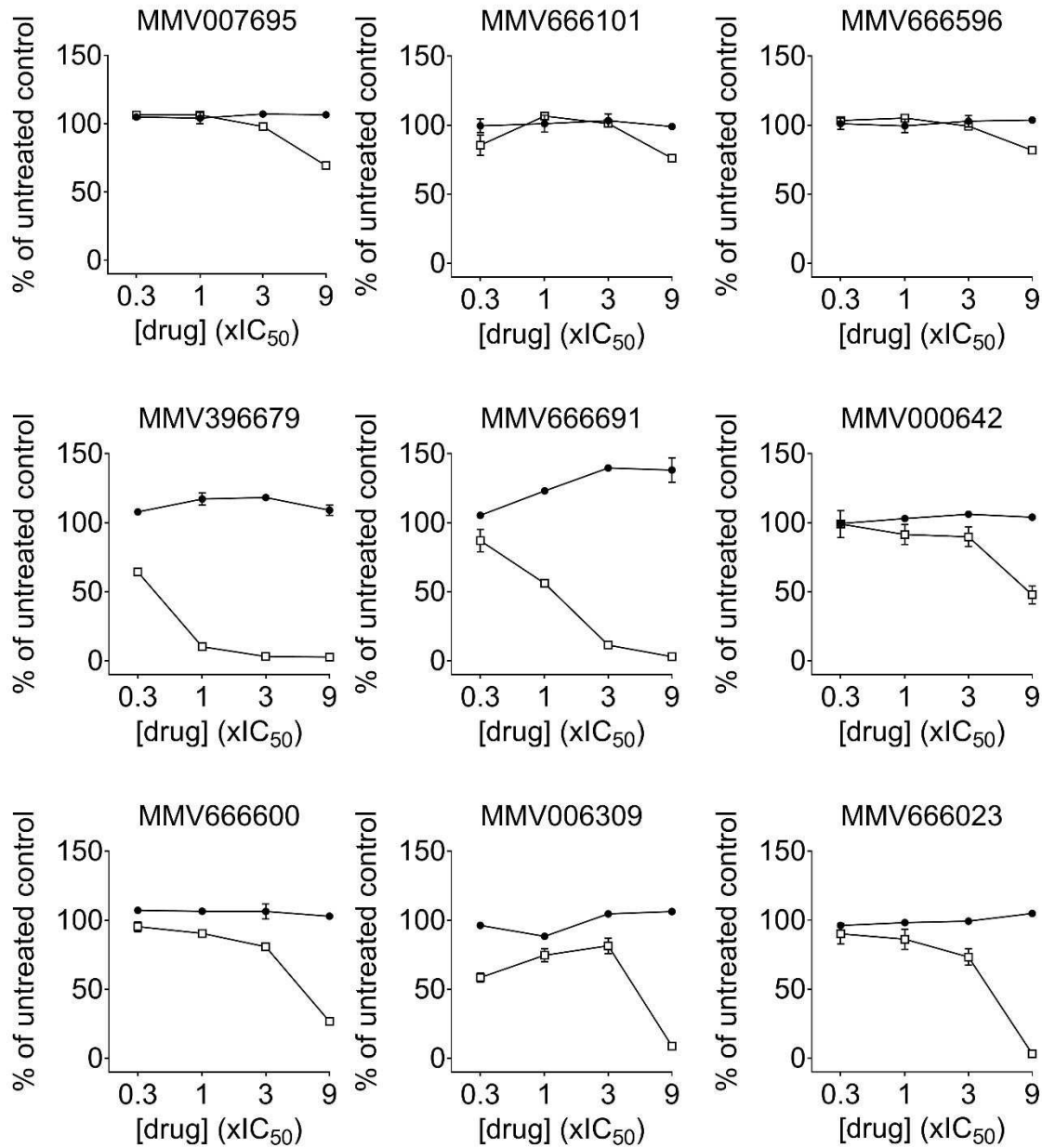D4

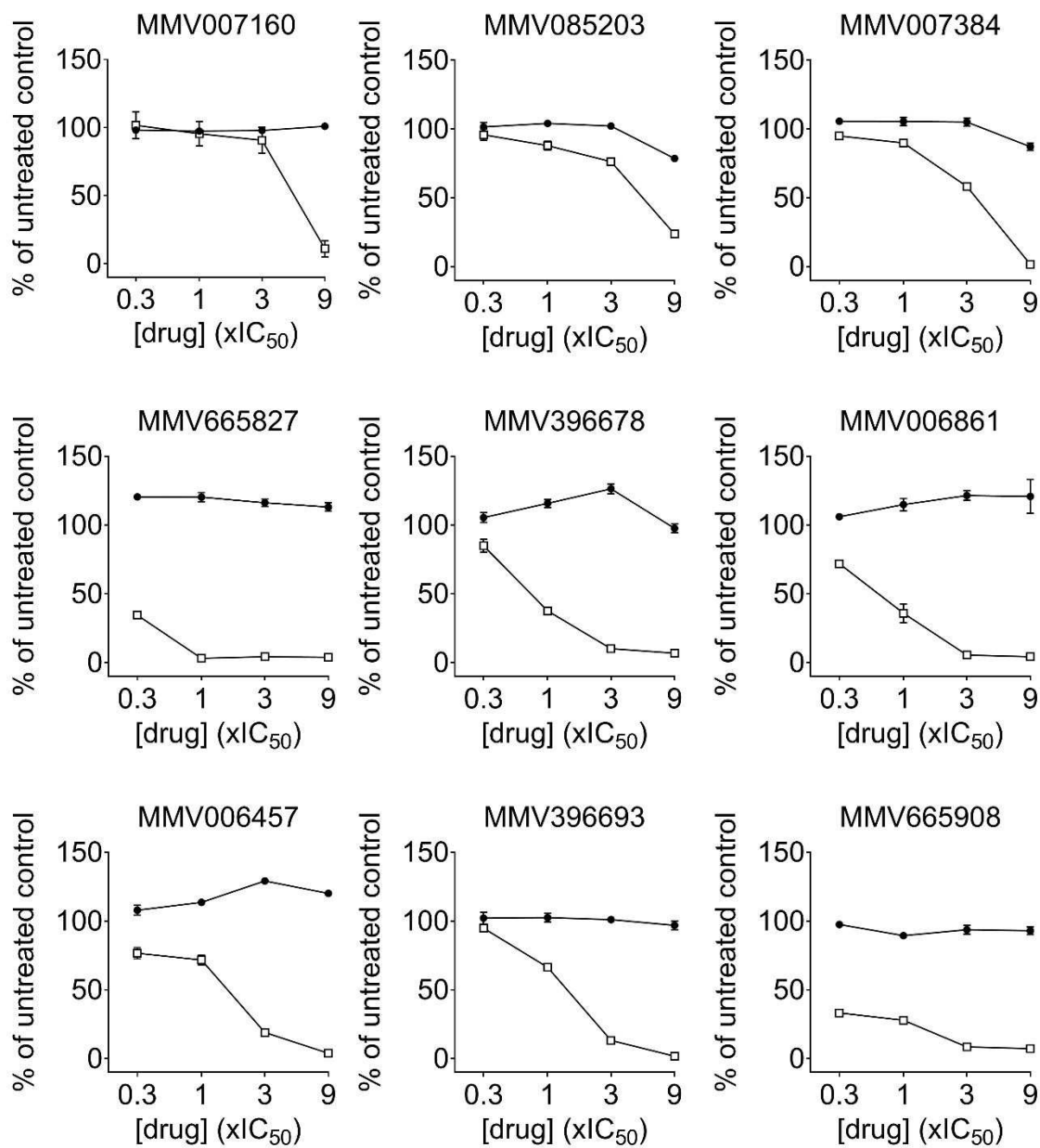# D5

D6

D7

D8

D9

D10
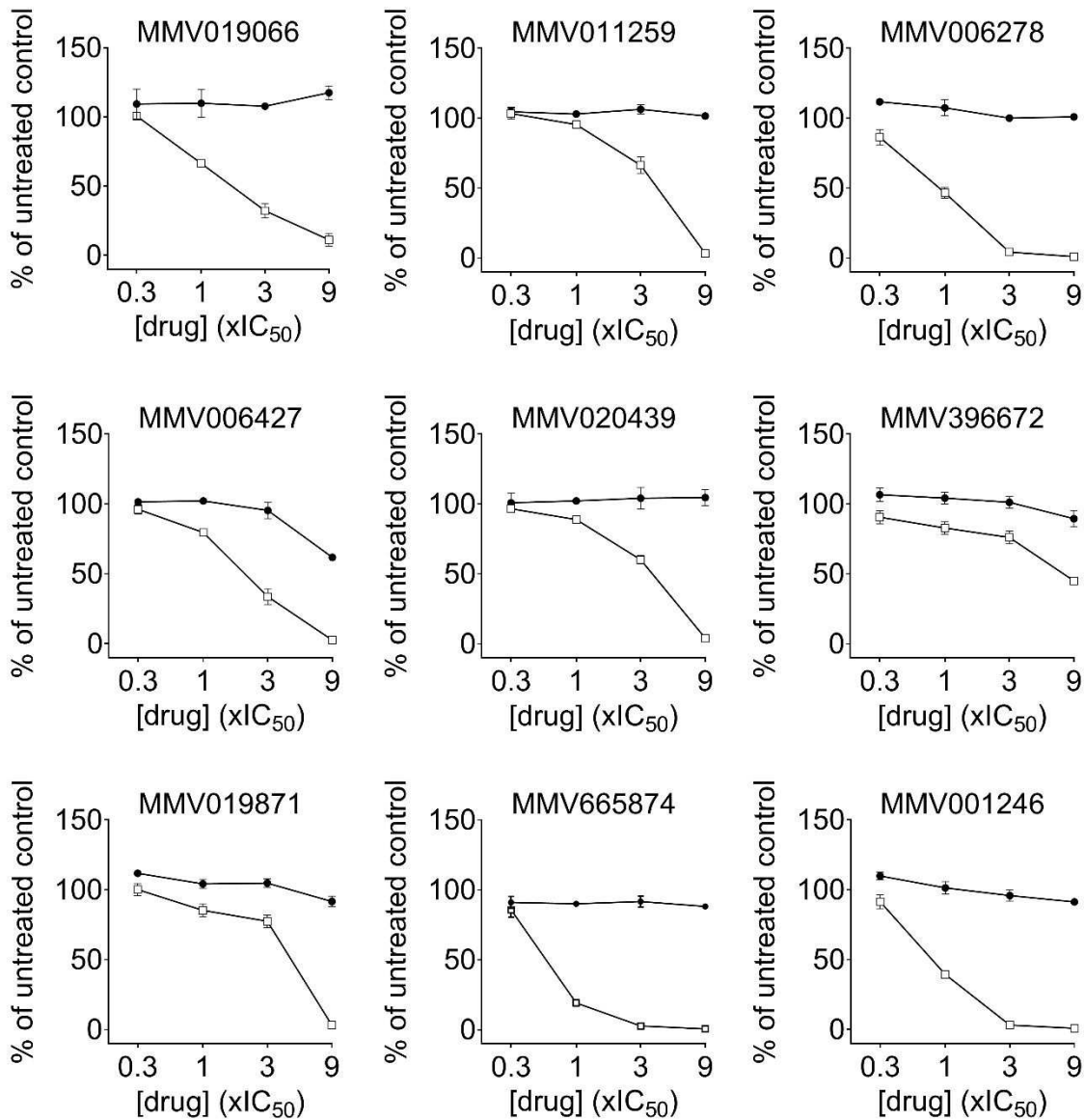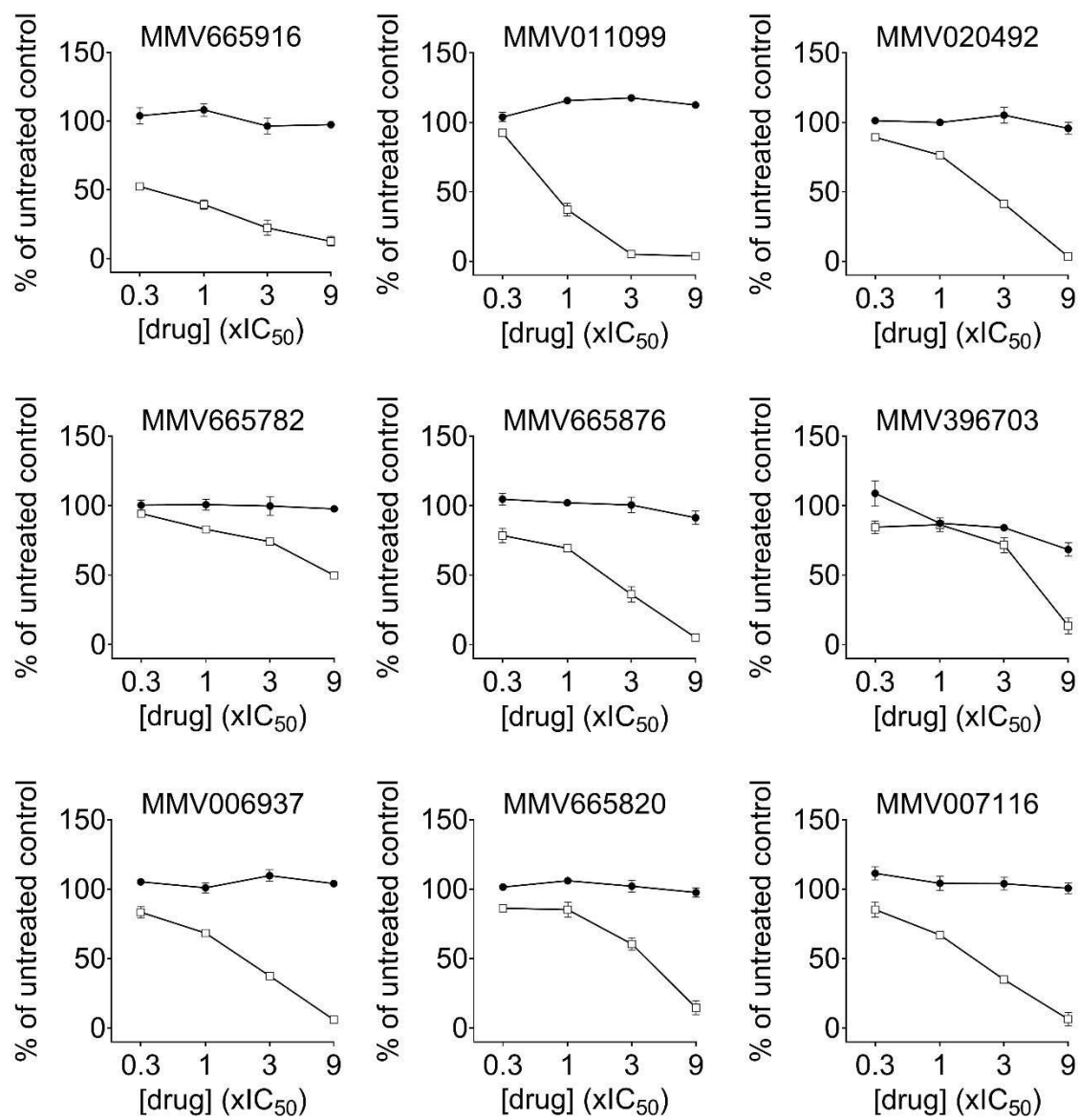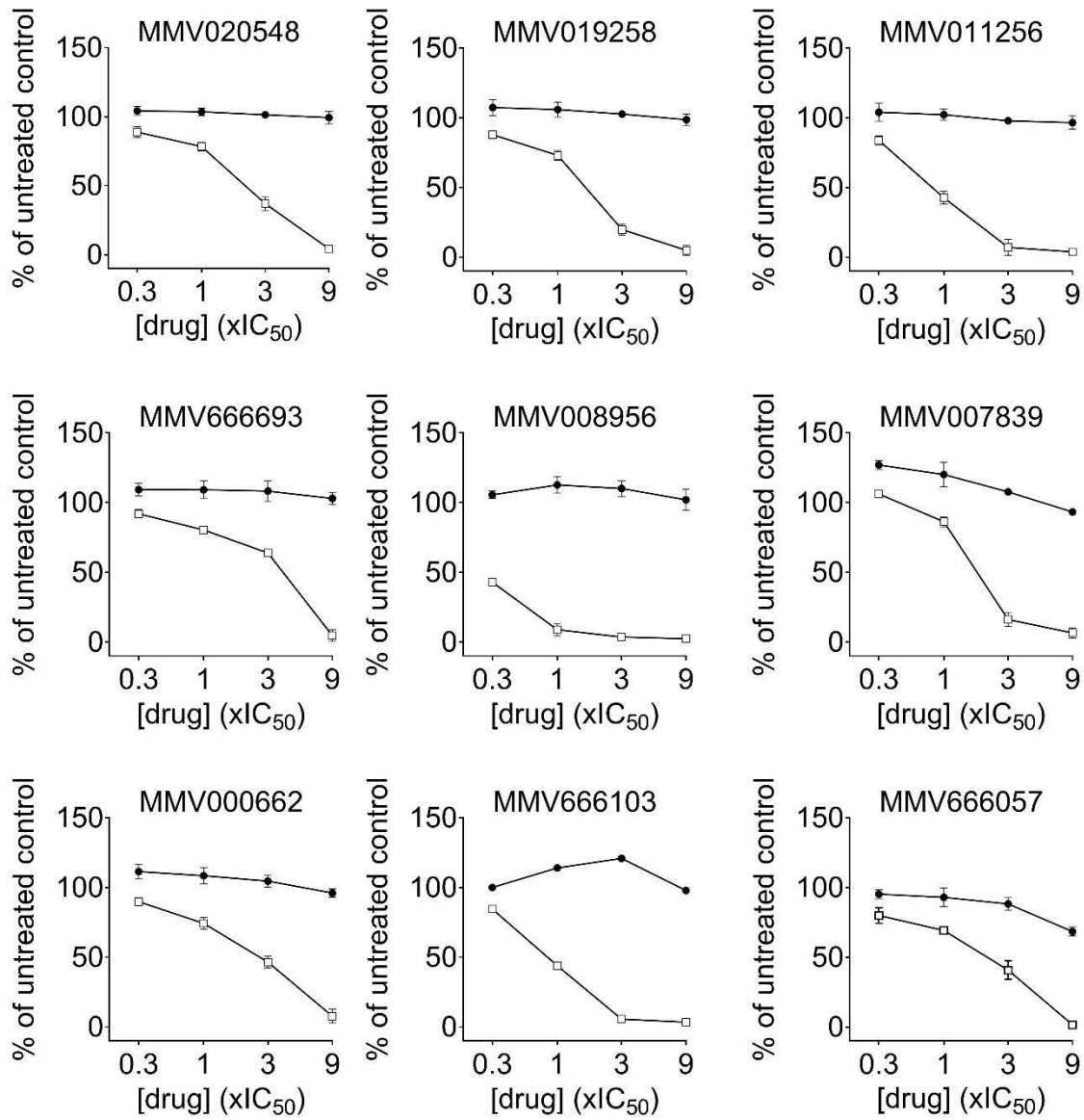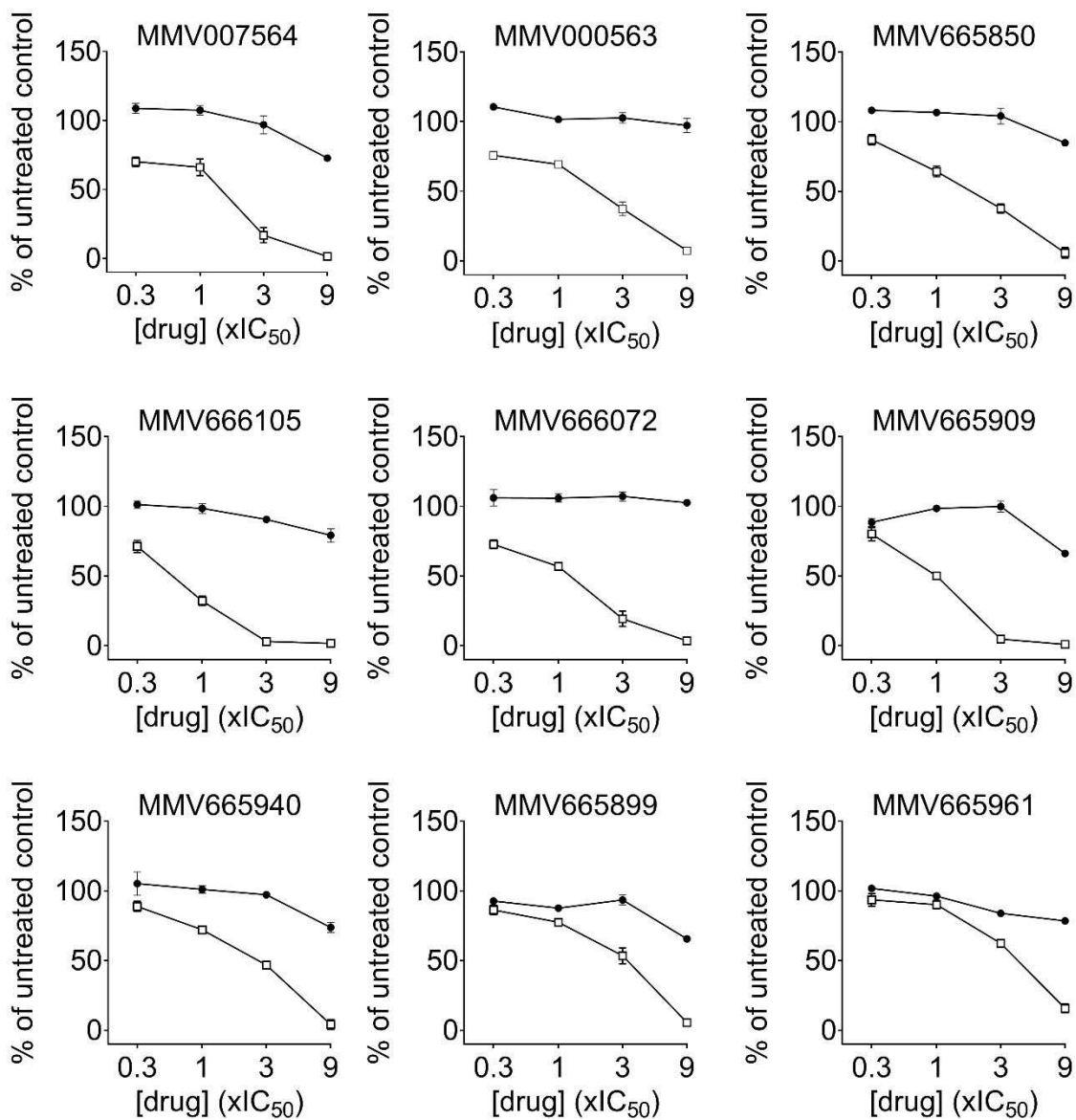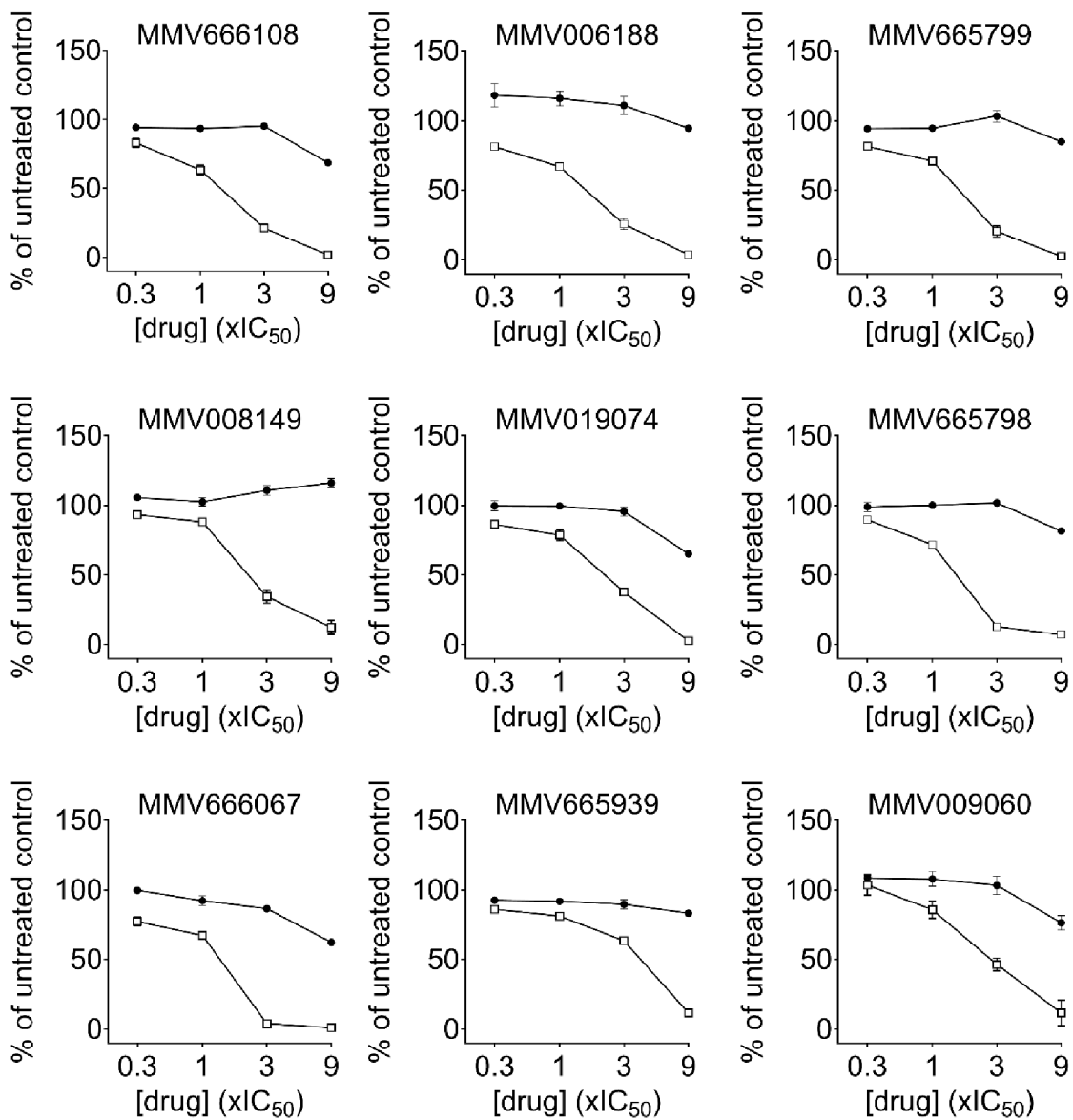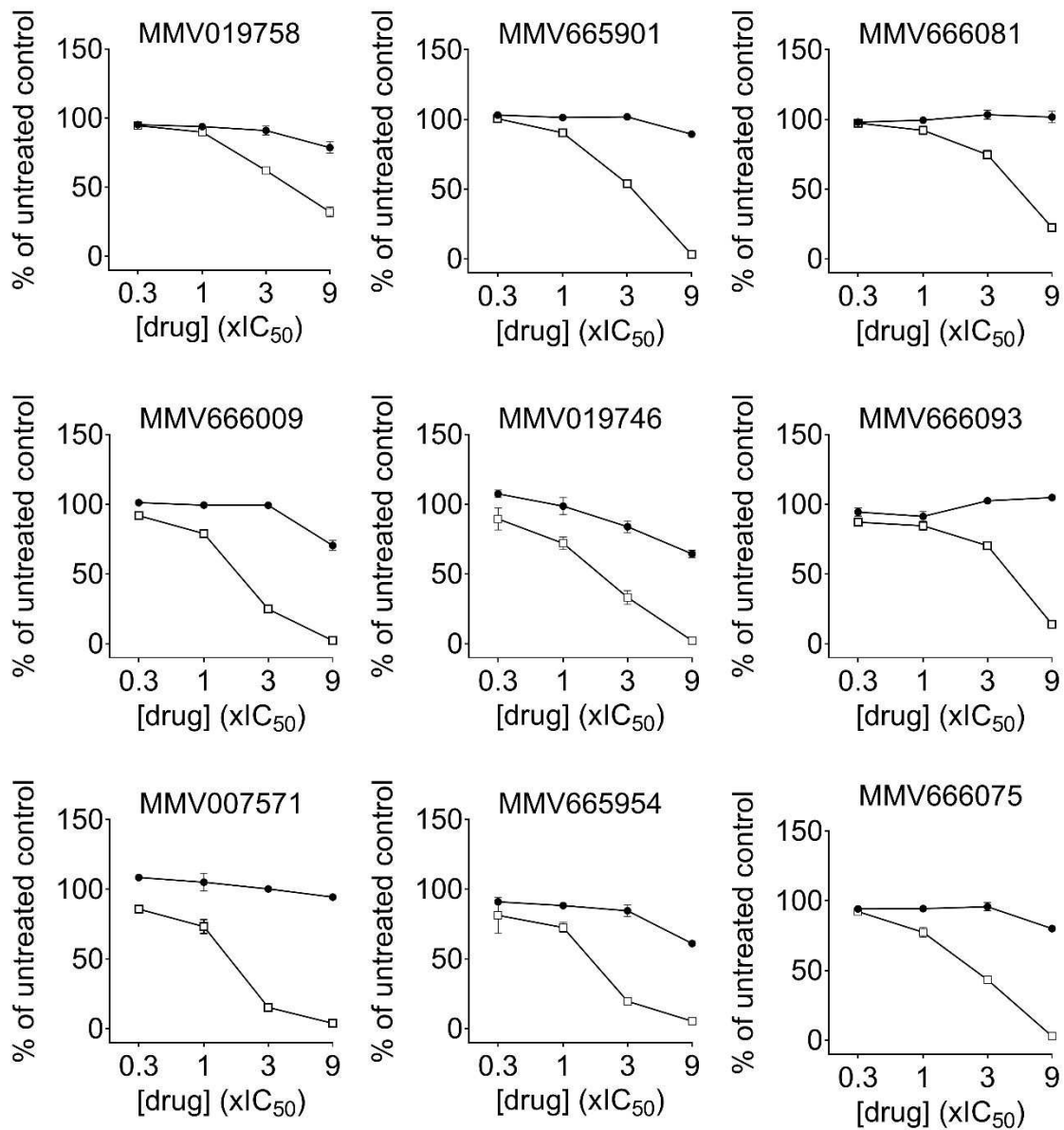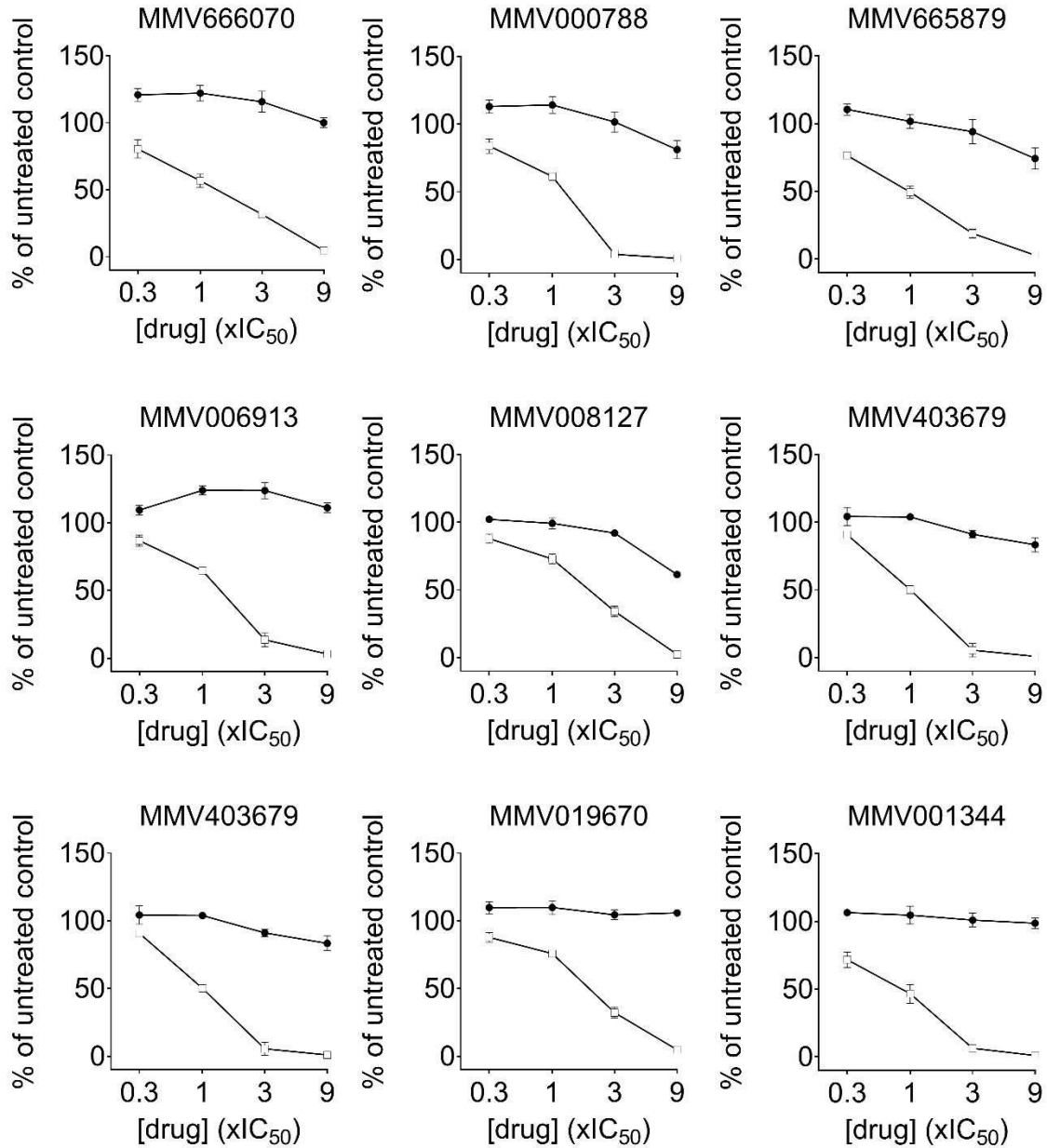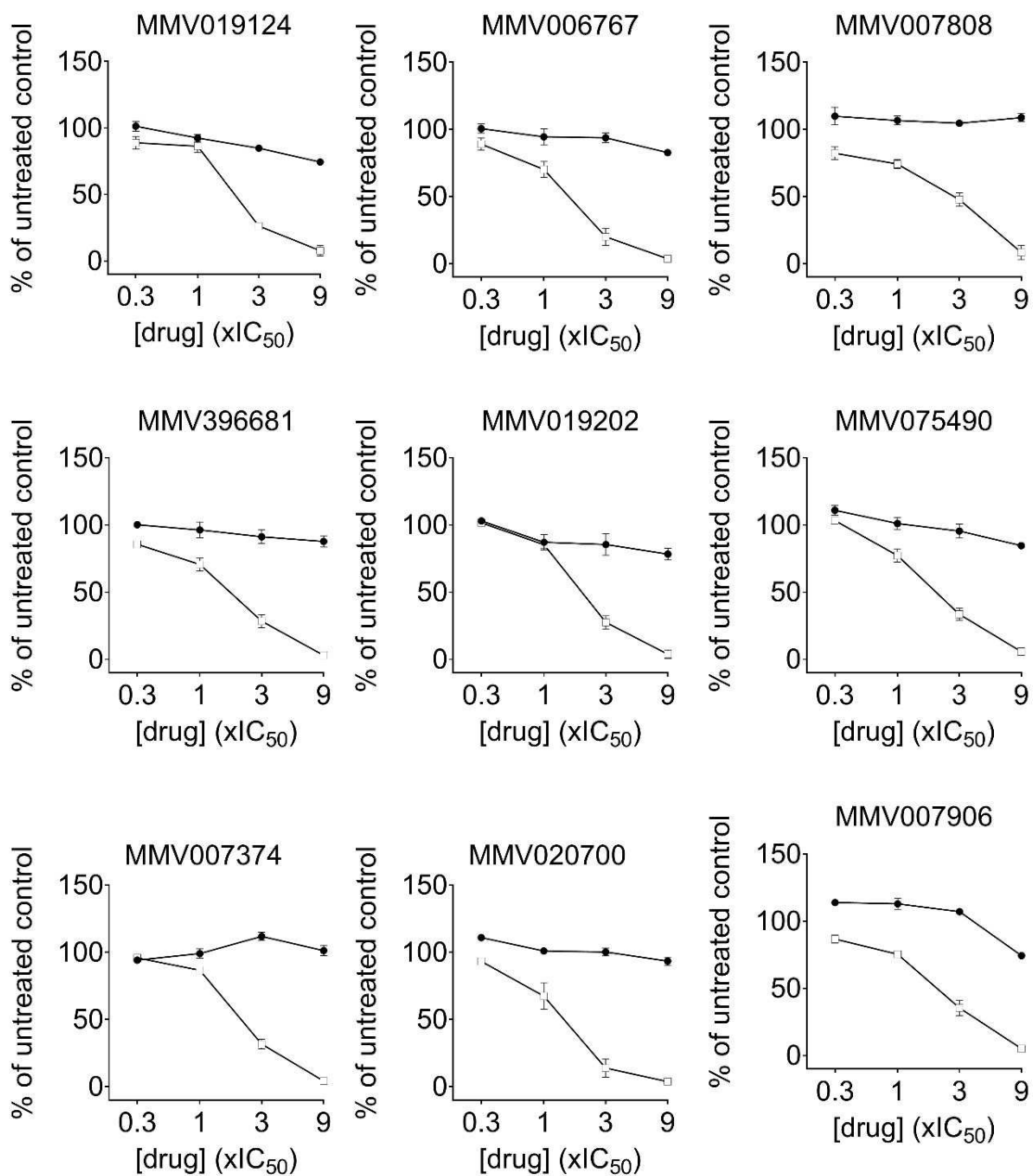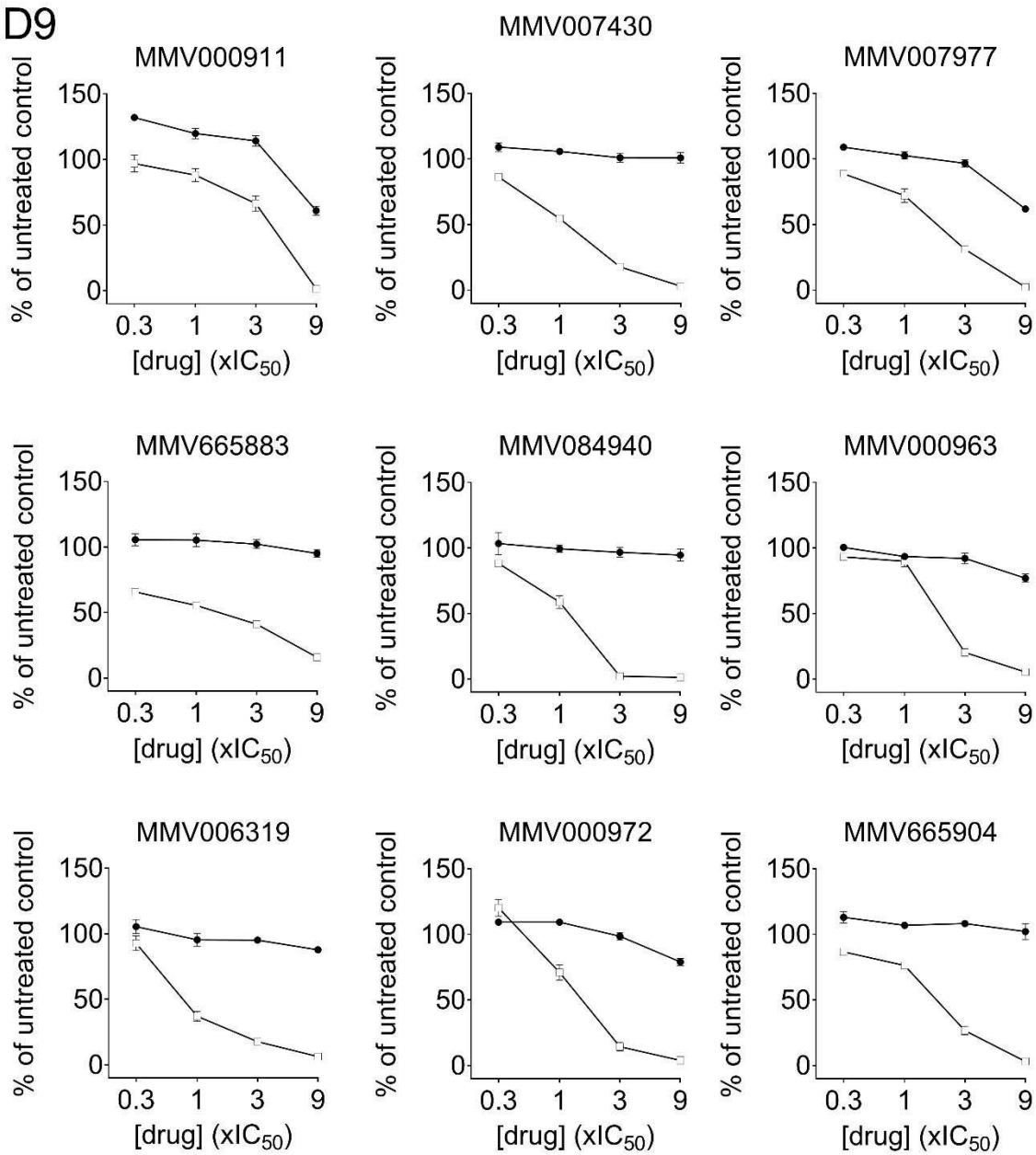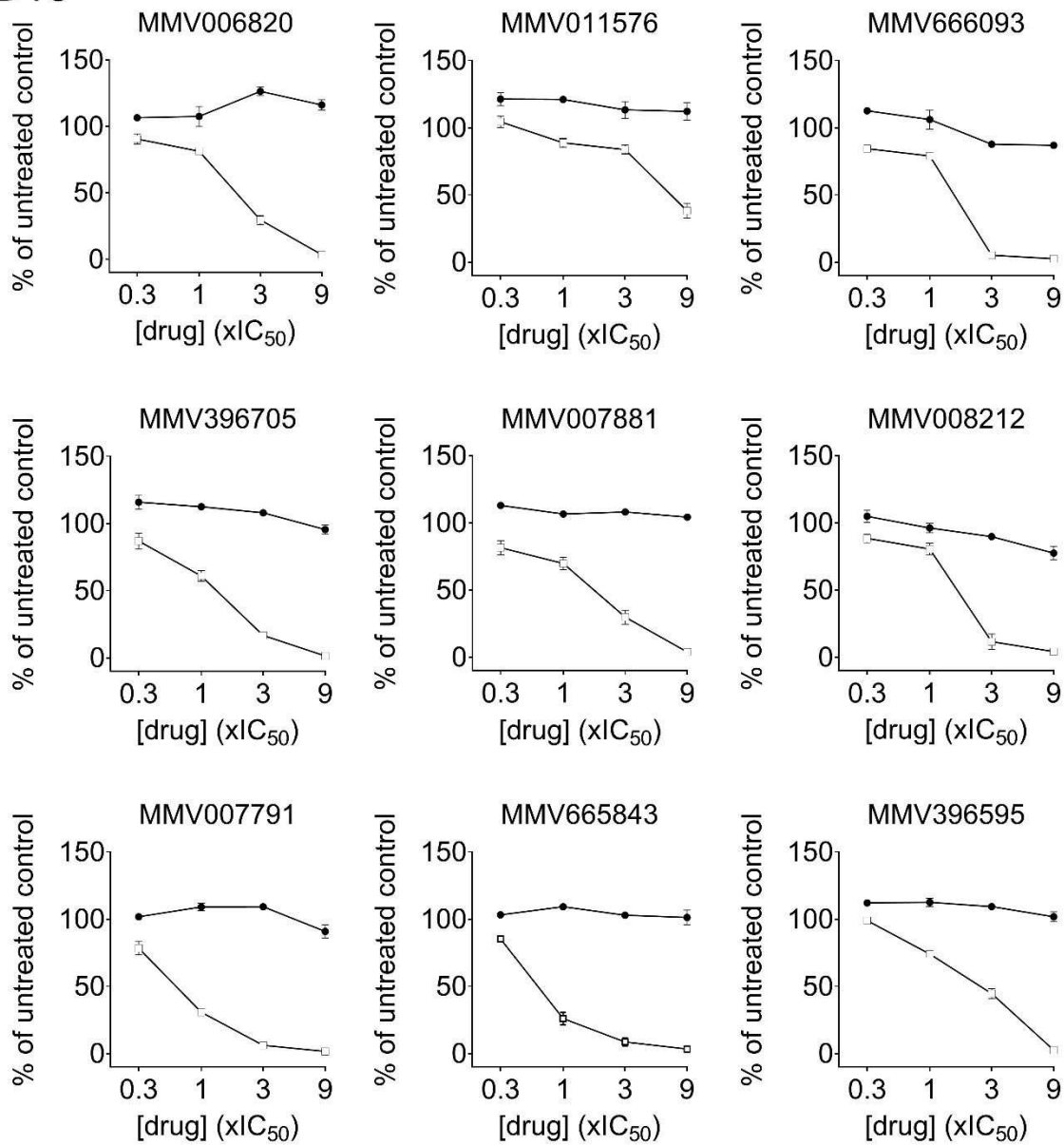
D11
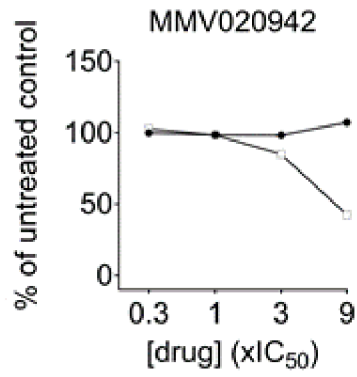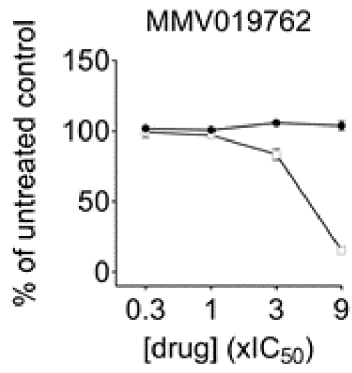
Figure S3. Equipotent-IC$_{50}$ concentration-dependent loss of bioluminescence plots for probe-like compounds screened from the MMV Malaria Box. The data for these probe-like compounds are shown on 10 panels (**P1-10**). The mean (error bars represent SD from three biological replicates) bioluminescence signal, normalised against an untreated control, remaining after a 6 h (closed circles) or 48 h (open squares) exposure to the indicated fold-IC$_{50}$ concentration of drug.
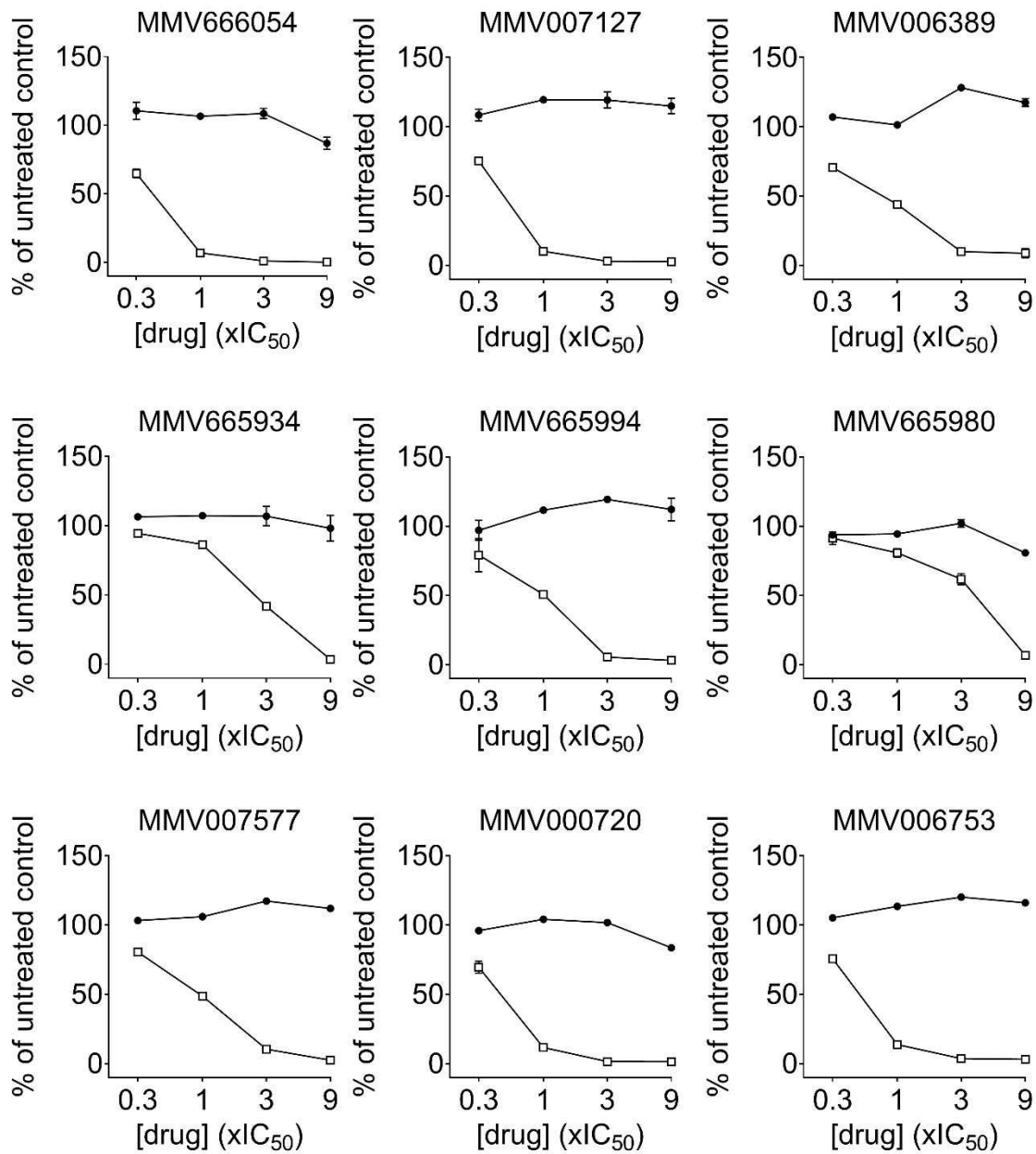
P2

P3

MMV007160

MMV085203

MMV007384

MMV665827

MMV396678

MMV006861

MMV006457

MMV396693

MMV665908

P4

P5

P6

P7

MMV665923

MMV007228

MMV073843

MMV667492

MMV007764

MMV665886

MMV396664

MMV086103

MMV084434

P8

P9

P10

MMV645672

MMV011438

MMV665840

MMV667489
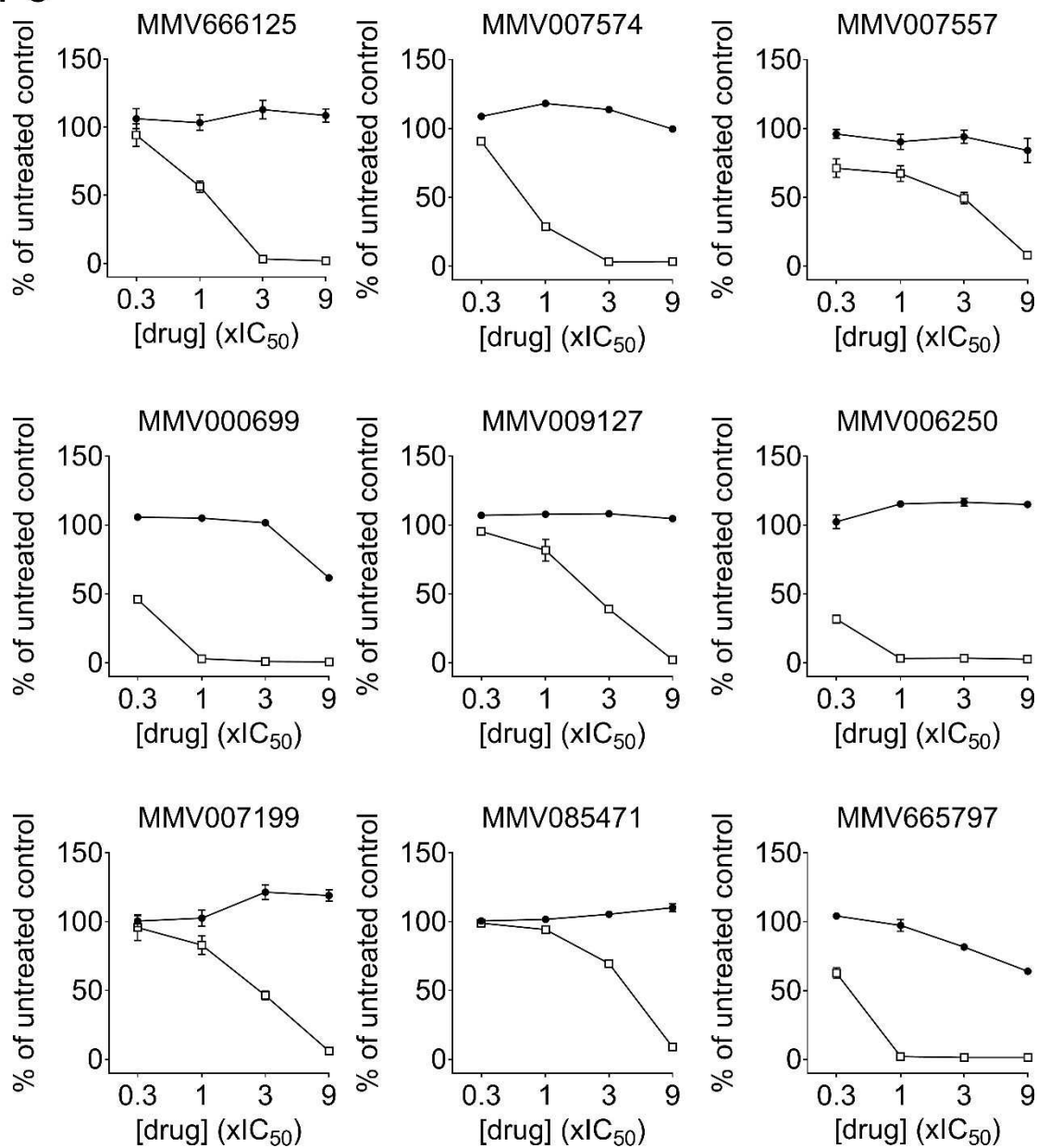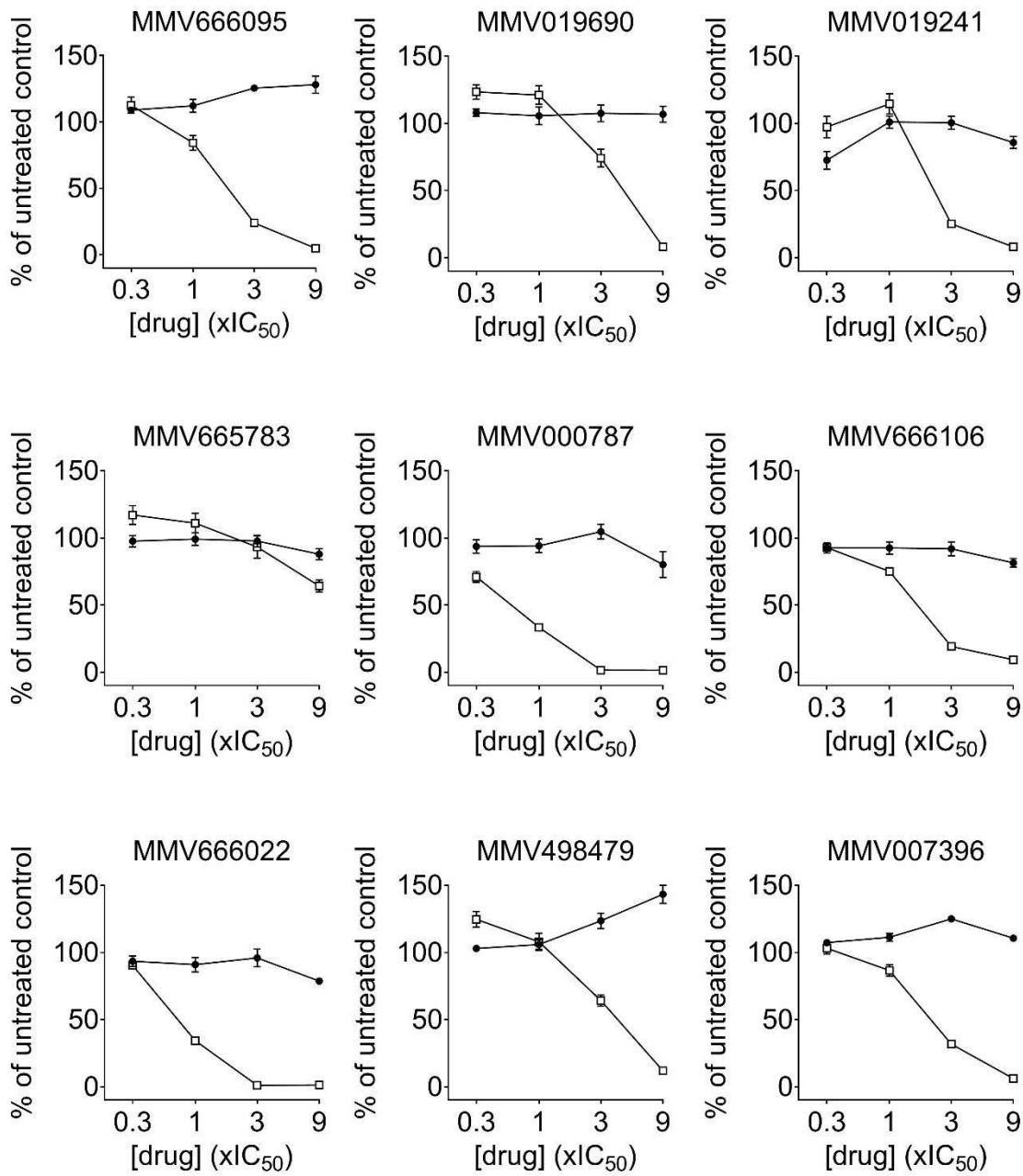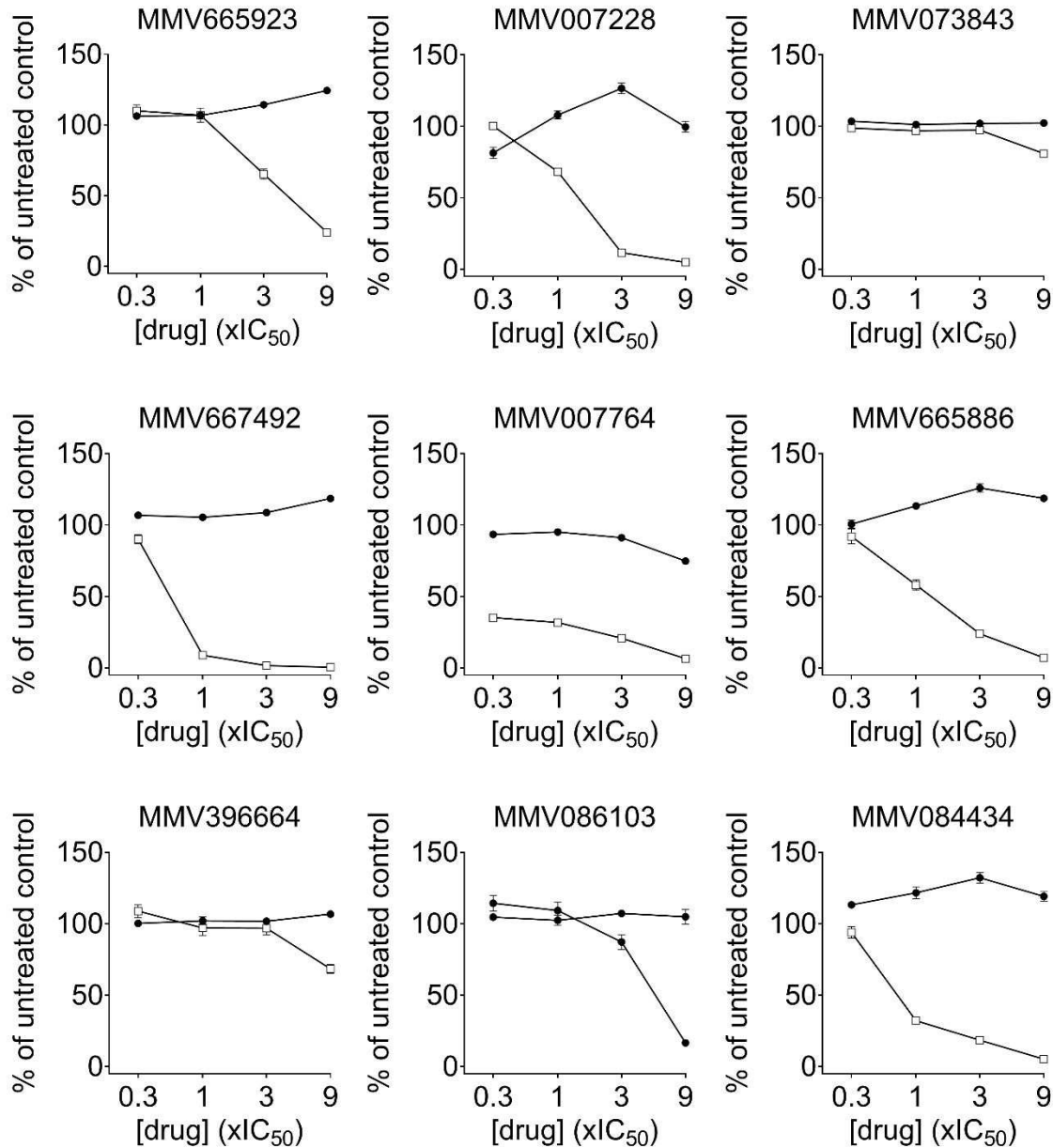
MMV396770

Details of Principle Components Analysis of 9xIC$_{50}$ to 0.33xIC$_{50}$ endpoints for 178 Malaria Box compounds

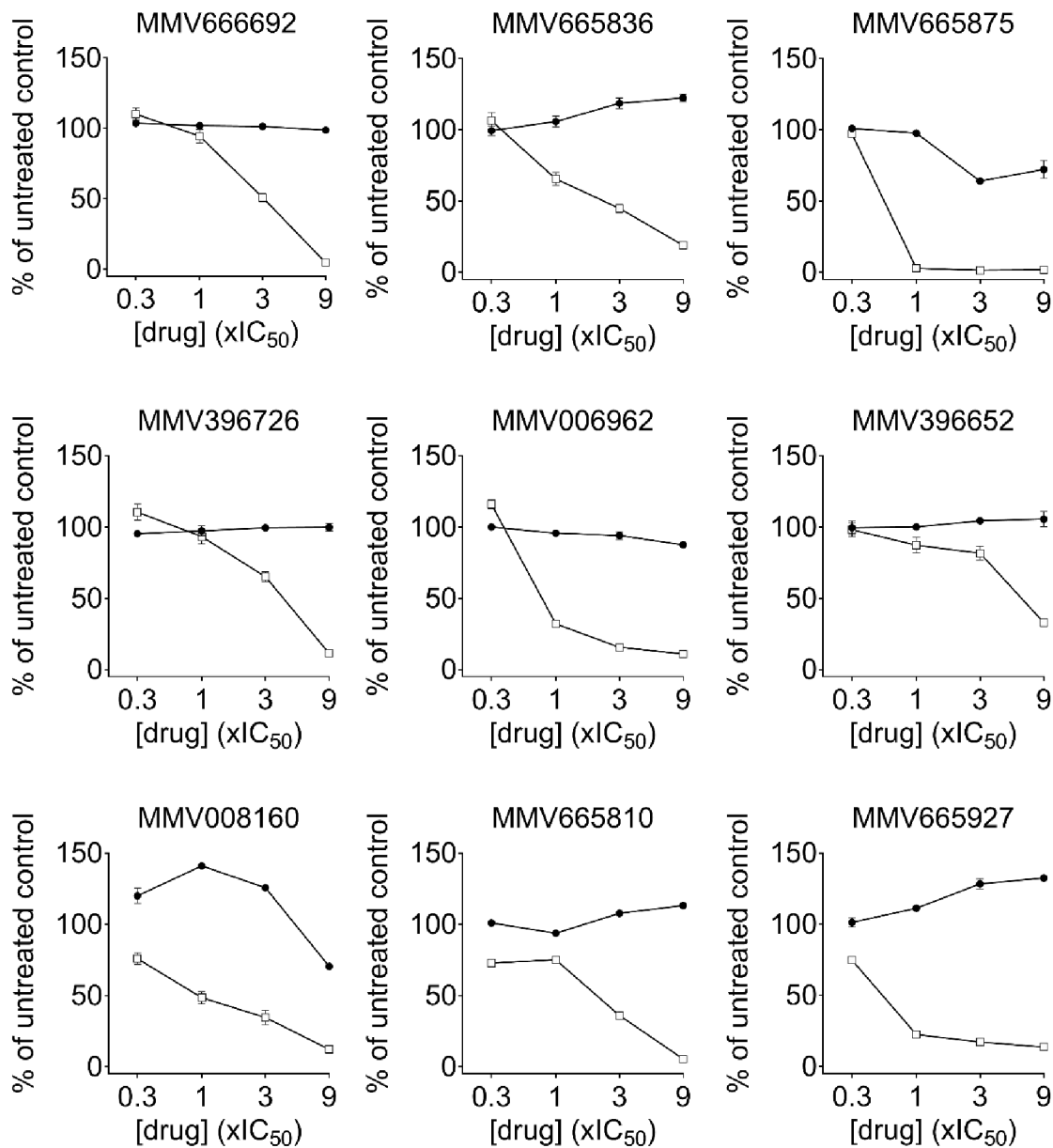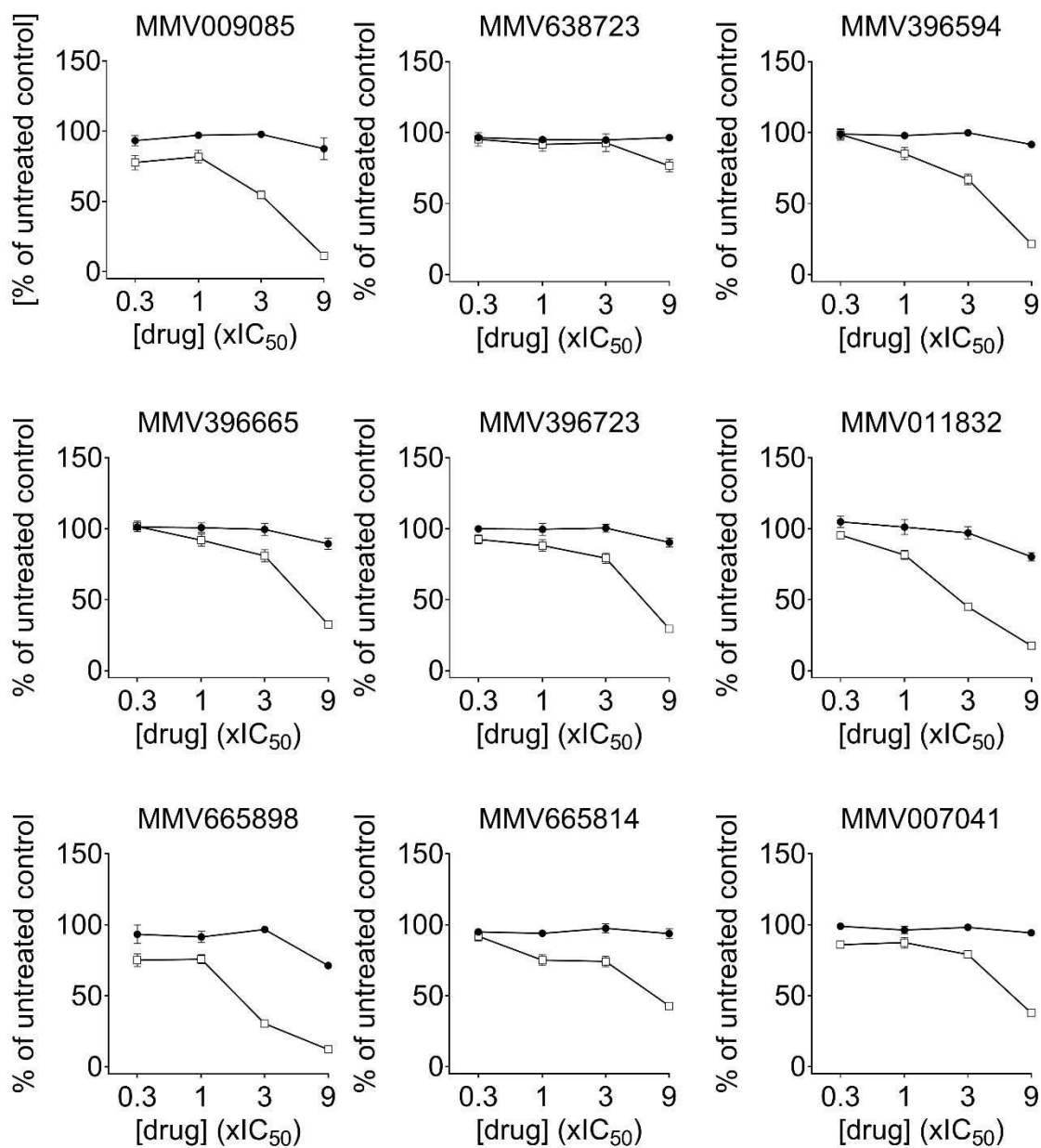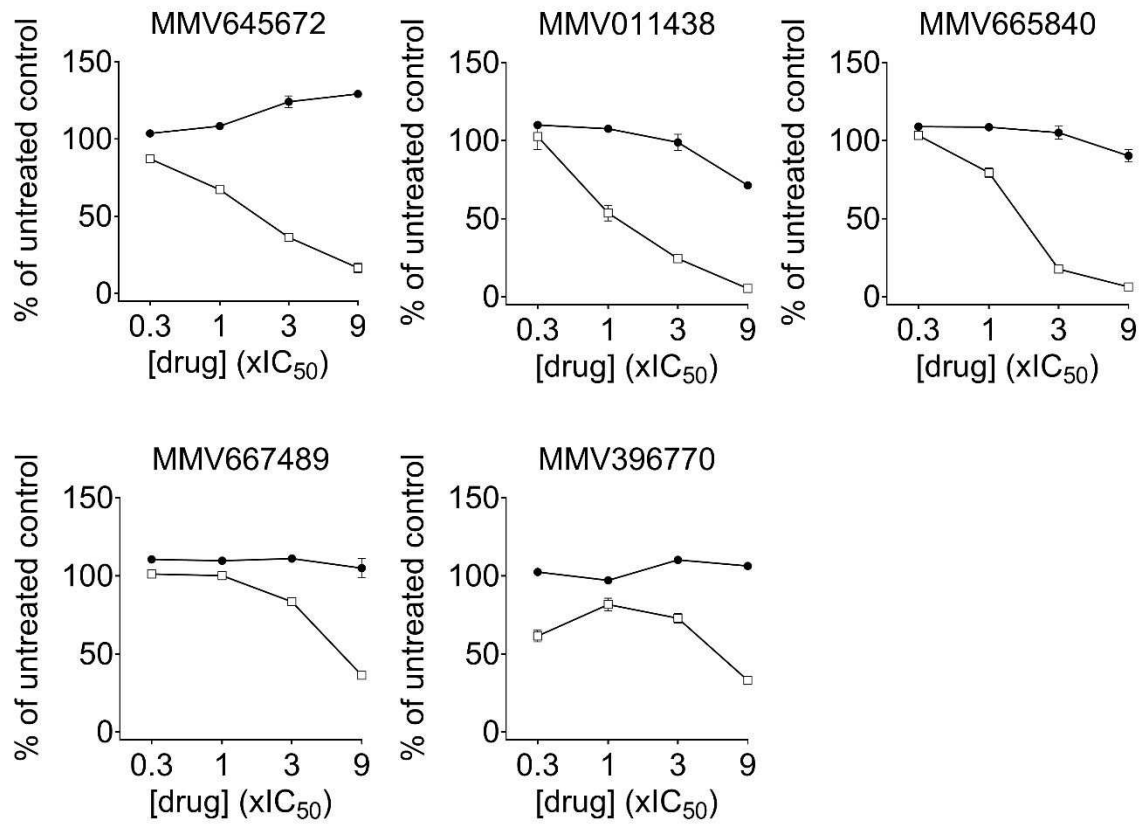Principle components analysis was performed on the 0.3x, 1x, 3x and 9x endpoints for BRRoK assessed at the 48 h timepoint using the KNIME analytics platform (https://www.knime.org/) to reduce the dimensionality of these data set, allowing the concentration-rate relationship to be captured in one parameter. This analysis reports that two principle components (PC1 and PC2) explain 92% of the variance in the parameters, with the first principle component explaining 78% of the total variance in the four original variables. A zero-meaned PC1 value was used to represent the BRRoK^{48hr} parameter.

Table S5. Eigenvalues and breakdown of % variance and cumulative variance explained by each principle component.

	Eigenvalue	% Variance explained	Cumulative variance explained
PC 1	1820.361	78	78
PC 2	319.7312	14	92
PC 3	130.3651	6	97
PC 4	68.0949	3	100

Table S6. Eigenvectors for each principle component showing the contribution (non-zero-meaned) that each 48 h BRRoK readout at different equipotent concentrations makes to the principle components.

BRRok Readout	PC1	PC2	PC3	PC4
9xIC$_{50}$	0.27	0.64	0.66	0.29
3xIC$_{50}$	-0.50	-0.50	0.45	0.55
1xIC$_{50}$	-0.51	0.09	0.44	-0.73
0.33xIC$_{50}$	-0.65	0.57	-0.42	0.27
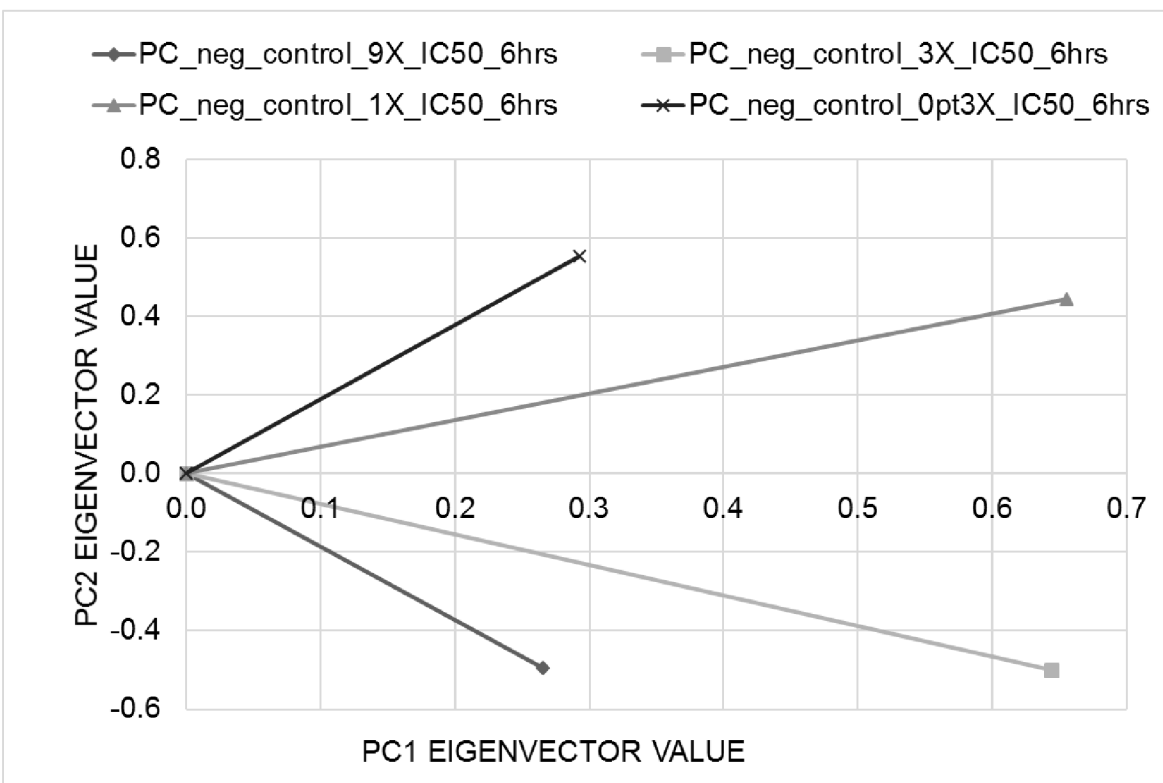
	9X	3X	1X	0.3X
9X	1.00			
3X	0.75	1.00		
1X	0.48	0.79	1.00	
0.3X	0.30	0.48	0.70	1.00

Figure S4. Spectral analysis of principle components showing that the foldxIC$_{50}$ BRRoK readout correlate positively with one another. The associated table below presents a correlation matrix for 9xIC$_{50}$ to 0.33xIC$_{50}$ BRRoK readouts (lower diagonal only shown to avoid repeating values about diagonal). Both the spectral analysis and correlation matrix reports that the BRRoK data produced at 9xIC$_{50}$ is most correlated with that at 3xIC$_{50}$. Generally, adjacent 3-fold dilution drug concentrations display the most correlation in BRRoK readout at 48 h.

Table S9. The range of all the biophysical properties seen in each set are summarized. Also, see table S7 for individual compounds data.

MW, molecular weight; LogP, log distribution coefficient; PSA, polar surface area ($Å^2$); RB, rotatable bonds; HBD/HBA, hydrogen bond

Property	All compounds tested in MMV-Box (370)		Fast MoA	Slow MoA	Fast Core	Slow Core
	PC1 <DHA	PC1>ATQ	*Pf*ATP4	bc_1	2-MAP	2-Ph-Bz
LogD	1 to 5.5	2 to 6.5	1 to 5	1-8	2-4	3-7
MW	250-400	250-500	300-450	200-600	250-400	350-500
PSA	<80	<90	=<90	=<80	=<60	=<90
RB	=<9	=<9	=<8	=<7	=<7	=<6
HBD	=<2	=<2	=<2	=<1	=<2	>=2
HBA	=<6	=<6	=<5	=<5	=<4	=<4
Fsp3	0.0 – 0.6	0.0 - 0.5	<0.45	<0.4	<0.65	<0.2
No. Rings	=<6	=<6	=<5	<5	<4	>=4
Basic pKa	<10	<10	<10	<5	<11	<7
Acidic pKa	>8	>6	>9	>9	>8	>10

donor/acceptor; Fsp3; fraction of sp^3 carbons; 2-MAP, 2-(Methylamino)-Phenols; 2-Ph-Bz, 2-PhenylBenzimidazoles

Table S10: Biophysical properties for compounds in the indicated modes of action. Also, see table S7 for individual compound data.

	PfATP4		Hgb catabolism		DHFR-TS		DHODH		bc$_1$	
	Fastest RoK	Slowest RoK	Fastest RoK	Slowest RoK	Fastest RoK	Slowest RoK	Fastest RoK	Slowest RoK	Fastest RoK	Slowest RoK
	MMV 396749	MMV 000642	MMV 142383	MMV 011576	MMV 006706	MMV 667486	MMV 666102	MMV 006937	MMV 665940	MMV 084434
MW	368.4	469	310.4	445	359.5	261	252.3	279.3	293.3	358.4
LogP	4.18	5.51	5.43	2.6	3.93	1.3	2.56	4.31	3.4	3.5
PSA	68	59	42	83	48	89	58	50	48	60
RB	1	6	3	6	2	3	2	1	4	4
HBD	2	1	1	6	0	2	2	1	0	1
HBA	4	3	2	1	4	3	3	3	3	5
Fsp3[1]	0.1	0.28	0.22	0.35	0.45	0.38	0.13	0.29	0.1	0.1
No. Rings	6	4	3	5	5	2	3	4	3	3
Basic pKa	<5	-	-	-	8.8	8.4	6.8	<5	-	-
Acidic pKa	-	-	-	-	-	-	-	-	-	-

MW, molecular weight; LogP, log partition coefficient; PSA, polar surface area (Å^2); RB, rotatable bonds; HBD/HBA, hydrogen bond donor/acceptor; Fsp3; fraction of sp^3 carbons

Additional Supplementary data

These Supplementary data files do not form part of the PDF but are available from the JAC Editorial Office (jac@bsac.org.uk) on request:

1. Table S2.xlsx

2. Table S3.xlsx

3. Table S7.xlsx

4. Table S8.xlsx